RIJKSINSTITUUT VOOR VOLKSGEZONDHEID EN MILIEUHYGIENE
BILTHOVEN

Rapport nr. 749202001

Ozone depletion and skin cancer incidence: an integrated modelling approach

H. Slaper, M.G.J. den Elzen, H.J. v.d. Woerd,
J. de Greef

June 1992

Dit onderzoek werd verricht in opdracht van Ministerie van VROM, Directoraat Generaal Milieubeheer, Directie Stoffen, Veiligheid en Straling

VERZENDLIJST

1 -	15	Ministerie van VROM; Directoraat Generaal Milieubeheer, Directeur Stoffen, Veiligheid en Straling
	16	Directeur-Generaal Volksgezondheid
	17	Directeur-Generaal Milieubeheer
18 -	20	plv. Directeur-Generaal Milieubeheer
	21	dr.ir. P. Vellinga, DGM/L
	22	drs. J. Swager, DGM/L
	23	drs. J.B. Weenink, DGM/L
	24	dr. L.H.J.M. Janssen, DGM/L
	25	prof.dr.drs.ir. O.J. Vrieze RU Limburg
	26	prof.dr. J.C. van der Leun, RUU afdeling Dermatologie
	27	dr. F.R. de Gruijl, RUU afdeling Dermatologie
	28	prof.dr. L. Reijnders, UvA Amsterdam
	29	drs. C. Kroeze, UvA Amsterdam
	30	dr.ir. T. Schneider, NOP Mond.Luvo en Klimaatverandering
	31	drs. S. Zwerver, NOP Mond. Luvo en Klimaatverandering
	32	drs. M. Berk, NOP Mond. Luvo en Klimaatverandering
	33	drs. M. Janssen, EUR, Rotterdam
	34	dr. W.F. Passchier, Gezondheidsraad
	35	prof.dr. D.P. Häder, Inst. für Botanik und pharmazeutische Biologie Erlangen
	36	dr. A. Webb, Dept. of Meteorology Reading, GB
	37	dr. M.G. Holmes, Univ. of Cambridge
	38	prof.dr. M. Tevini, Univ. Fridericiani
	40	dr. L. Grant EPA/USA
	41	Depot van Nederlandse publicaties en Nederlandse bibliografie
	42	Directie RIVM
	43	Hoofd Voorlichting & Public Relations
	44	Directeur Sector Milieuonderzoek (VII)
	45	Directeur Sector Toekomstverkenning (IV)
	46	Hoofd van het Laboratorium voor Stralingsonderzoek
	47	Informatie- en Documentatiecentrum Laboratorium voor Stralingsonderzoek
	48	dr. R.M. van Aalst
	49	drs. A. van der Giessen
	50	dr. P.G.M. Kramers
	51	prof.dr. H.A.M. de Kruijf
	52	drs. R.M.J. Maas
	53	dr. F.A.A.M. de Leeuw
	54	ir. R.J. Swart
	55	prof.dr.ir. J. Rotmans
	56	drs. G.J. Eggink
	57	dr. H. Reinen
58 -	118	Auteur(s)
	119	Bureau Projecten- en Rapportenregistratie
	120	Bibliotheek RIVM
121 -	130	Reserve-exemplaren

TABLE OF CONTENTS

ABSTRACT

A decrease in stratospheric ozone, probably caused by chlorofluorocarbon (CFC) emissions, has been observed over large parts of the globe. Further depletion is expected and has led to growing public concern regarding the possible adverse effects. Stratospheric ozone is the primary atmospheric absorber of biologically effective solar UV, and thus (partly) protects against various harmful UV-effects. The incidence of skin cancer, already one of the most common types of cancer among Caucasian populations, is expected to increase due to ozone depletion. An integrated source-risk model is developed and applied to evaluate the increased skin cancer incidence related to various CFC emission scenarios. The source-risk model consists of a series of submodules describing the various aspects of the source-risk chain, and is an independent submodule within the framework of IMAGE, an integrated source-effect-model for climate change and ozone depletion.

The model provides estimates for tropospheric concentrations of CFC's, chlorine levels in the stratosphere, ozone depletion, UV irradiance and effects on skin cancer incidence and death rates. The model results show that no full recovery of the stratospheric chemical balance is expected, even if all countries in the world were to comply to the London Amendments of the Montreal Protocol.

Excess death and incidence rates refer to the additional skin cancer cases caused by ozone depletion. In the Netherlands the excess death rate is estimated to increase from 1.5 per million per year around 2000 (for all scenarios considered) to 2-4 per million per year around 2050 if the London Amendments are fully implemented, and 6-10 per million per year if the Montreal Protocol is adopted worldwide. After 2050 a slight decrease will occur in the excess death rate estimations for the London Amendments (1-2 per million per year in 2100). The results for the Montreal Protocol show a continuous increase in excess death rates throughout the entire century, leading to 11-18 per million per year by 2100.

Averaged over the period 2000-2050, the yearly excess death and incidence rates are lower by nearly twofold for the London Amendments as compared to the Montreal Protocol. For the Dutch population, the estimates are: 2.7 versus 5.3 deaths per million per year, 5.4 versus 10.2 melanoma cases per million per year and 200 versus 395 nonmelanoma skin cancer cases per million per year.

Comparing the estimates for the Netherlands with preliminary estimates for the USA shows that for all scenarios excess mortality rates averaged over the period 2000-2050 will be 20-25% higher in the USA, excess incidence rates for melanoma will be 10% lower, and for non-melanoma 55% higher.

Rough estimates for the global implications in the period 2000-2050 show that for the Montreal Protocol 3300 additional deaths, 4600 excess cases of melanoma and over 300,000 cases of non-melanoma are expected per year. Full implementation of the London Amendments reduces these estimates approximately twofold. These global estimates are probably conservative.

The volcanic eruption of the Pinatubo in 1991 could enhance the ozone depletion caused by CFC's over a limited time period. A preliminary upper estimate of the possible effect on the excess skin cancer death rate in the Netherlands is 0.4-0.5 per million per year for around 2000 (slowly decreasing afterwards).

The model can be used to evaluate the effects of various new policy options, including the role of CFC alternatives. Furthermore, the model can also be applied for estimating other effects of UV exposure if sufficient information on the exposure-effect relationships becomes available.

SAMENVATTING

Wereldwijd is aantasting van de stratosferische ozonlaag waargenomen, die waarschijnlijk het gevolg is van de emissie van chloorfluorkoolwaterstoffen (CFK's). De verwachting is dat de ozonaantasting voortzet. Dit leidt tot verontrusting over de mogelijke gevolgen voor mens en milieu. Stratosferisch ozon absorbeert een belangrijk gedeelte van de schadelijke UV-straling van de zon, en tempert aldus de schadelijke effectiviteit van zonlicht. Eén van de schadelijke gevolgen van een aantasting van de ozonlaag is de te verwachten toename van het aantal gevallen van huidkanker, één van de meest voorkomende vormen van kanker in blanke populaties. Om de gevolgen van ozonaantasting op de incidentie van huidkanker te schatten is een geïntegreerd bron-risico-model ontwikkeld en toegepast. Het bron-risico model beschrijft de complete keten van produktie en emissie tot en met het effect op de incidentie van huidkanker, en is opgebouwd uit een zevental modulen. Het gehele model is een onafhankelijke module, die past binnen het kader van het IMAGE-model, een geïntegreerd bron-effect-model voor klimaatverandering en aantasting van de ozonlaag.

Met het model zijn op basis van verschillende CFK-emissiescenario's schattingen gemaakt van troposferische concentraties van CFK's, van chloride niveau's in de stratosfeer, ozon afbraak, UV-toename en effecten met betrekking tot huidkanker incidentie en sterfte. De modelresultaten laten zien, dat ook bij wereldwijde toepassing van de London Amendments op het Montreal Protocol, er geen volledig herstel van de stratosferisch chemische balans te verwachten is.

De studie is gericht op het schatten van toegevoegde risico's. Hieronder vallen uitsluitend de extra gevallen ten gevolge van de ozonaantasting. Voor Nederland wordt geschat dat voor alle scenario's het toegevoegde sterfte risico rond het jaar 2000 uitkomt op 1,5 per miljoen per jaar. Daarna wordt tot 2050 een toename van het toegevoegde sterfterisico verwacht tot 2-4 per miljoen per jaar voor het London Amendments scenario, en 6-10 per miljoen per jaar voor het Montreal Protocol. Na 2050 volgt voor het London Amendments scenario een geringe teruggang tot 1-2 per miljoen per jaar in 2100, en een verdere toename tot 11-18 per miljoen per jaar in 2100 voor het Montreal Protocol.

Gemiddeld voor de periode van 2000-2050 zijn de toegevoegde risico's voor het London Amendments scenario bijna tweemaal lager dan voor het Montreal Protocol. Voor de Nederlandse populatie geven de schattingen 2.7 tegen 5.3 doden per miljoen per jaar, 5.4 tegen 10.2 melanoom gevallen per miljoen per jaar, en 200 tegen 395 huidcarcinoom gevallen per jaar.

In vergelijking met de toegevoegde risico's voor Nederland geeft een voorlopige schatting voor de Verenigde Staten aan dat voor alle scenario's het gemiddeld over de periode 2000-2050 toegevoegd sterfterisico 20-25 % hoger ligt dan in Nederland, voor de toegevoegde melanoom incidentie 10% lager en voor de huidcarcinomen 55 % hoger.

Een ruwe schatting voor wereldwijde gevolgen geeft aan dat gemiddeld over de periode 2000-2050 wereldwijd een extra sterfte van 3300 personen per jaar wordt geschat ten gevolge van 4600 extra melanoom patiënten per jaar en 300000 huidcarcinoom patiënten. Deze cijfers moeten als conservatief worden aangemerkt.

De vulkanische uitbarsting van de Pinatubo in 1991 kan de ozonafbraak mogelijk enige jaren versnellen. Een bovenschatting van de mogelijke effecten levert maximaal 0,4-0,5 extra sterfgevallen per miljoen per jaar rond het jaar 2000 en een geleidelijke afname daarna.

Het model kan gebruikt worden voor de evaluatie van nieuwe beleidsopties. Uitbreiding naar andere effectgebieden is mogelijk, indien voldoende informatie over dosis-effect relaties beschikbaar is.

1 INTRODUCTION

Ultraviolet radiation (UV) has many effects on human health and the environment (UNEP, 1989; UNEP, 1991). The negative health effects of UV exposure are: skin ageing, skin cancer, erythema, cataracts, keratitis and most probably immuno suppression. Negative side effects of increases in UV exposure on plants relate to reduced growth, with possible negative implications for agricultural crops; furthermore, changes in competitive balances in ecosystems are expected. In aquatic ecosystems a reduction of primary producers (phyto-plankton) could have negative consequences for the aquatic food chains and thus for fisheries.

The sun is the primary source of UV exposure (Slaper and Eggink, 1991). The shorter wavelengths in the solar spectrum are most effective. These wavelengths, often referred to as UV-B (280-315 nm), are strongly scattered and absorbed in the earth's atmosphere. Ozone is the primary absorber of UV-B in the atmosphere and serves as a protective shield against too high intensities of harmful UV. Most of the atmospheric ozone is situated in the higher atmosphere, the stratosphere, and more specifically in a layer between 20 and 40 km above the earth's surface. This layer is often referred to as the ozone layer.

Concern about a possible depletion of the ozone layer arose in the early 1970s, when it was realised that human activities could lead to a disturbance of the physical and chemical balances that are responsible for the constant production and destruction of atmospheric ozone. Primary focus was on chlorofluorocarbons (CFC's), although (supersonic) air travel and space flights were also suspected contributers to ozone depletion. CFC's are used in aerosol propellants, refrigerants, solvents, foam blowing agents and in many other industrial processes. CFC's have long atmospheric lifetimes and can disperse to the stratosphere where photodissociation leads to a release of chlorine, which enters a catalytic process destroying ozone molecules. Rising concern for the environmental threat of a depleting ozonelayer led to a ban of CFC's in non-essential aerosols in the USA and the (West) European countries in the years 1974-1978.

In 1985 the Antarctic ozone hole was discovered. More than 50% ozone loss occurred over the Antarctic in the early spring. The Antarctic ozone hole was closely related to increases in active chlorine in the stratosphere. In recent years further evidence has been gathered to show that depletion occurred not only at the Antarctic, but also at midlatitudes in both the northern and the southern hemispheres (Stolarski et al., 1991). The observed depletion rate exceeds model prognosis.

Following the discovery of the Antarctic ozone hole UNEP initiated an international conference on the Protection of the Ozone Layer. This led in 1987 to a protocol aiming at a restriction of CFC emissions, the Montreal Protocol (UNEP, 1989). In view of the unexpectedly high depletion rate, more restrictive amendments to the Montreal protocol were proposed, aiming at a complete ban of the most important ozone-depleting substances by the year 2000 (London Amendments 1990) (UNEP, 1991). The EC countries agreed on a complete stop of the production for 1997.

Despite these efforts it is clear that ozone depletion has occurred over the past decade and due to the fact that many ozone-depleting substances have long atmospheric lifetimes, there is general agreement that depletion will continue. This is further emphasised by the surprisingly

high stratospheric concentrations of active chlorine in large parts of Europe and the USA, as reported in February 1992 (NASA, 1992). New policy options are under discussion, including the role of alternatives. Several goverments have adopted risk-oriented approaches on environmental policies aiming at a reduction of adverse effects of environmental pollution through source-directed countermeasures (VROM, 1989; EPA, 1990). Regarding the adverse effects of ozone depletion, several questions arise. To what extent will these effects occur and how are adverse effects influenced by various production scenarios?

Our aim was to develop an integral prognostic source-effect model to serve as a tool to support risk-oriented policy approaches regarding ozone depletion and to support decision-making in relation to risk limitation and sustainable development. The model developed in this study combines and integrates results from various research areas, i.e. atmospheric chemistry, atmospheric optics and biological dose-effect modelling. The model can be applied to obtain a full quantitative evaluation of the source-effect chain and consists of seven submodules covering the various aspects of the source-effect chain. At present the effect module is limited to the evaluation of skin cancer risks. The model itself is a separate independent submodule in the framework of IMAGE, an integrated source-effectmodel for climate change and ozone depletion (Rotmans, 1990). The model developed in this study is used to estimate effects of various CFC emission scenarios on skin cancer incidence. We realise that skin cancer is not the only, and possibly not the worst, effect of ozone depletion (UNEP, 1991). However, skin cancer plays a major role in the public concern, and is the major effect for which quantification of risks is possible at present.

Skin cancer is one of the most common forms of cancer among Caucasians. The yearly incidence in the Netherlands is estimated to be 15,000-18,000; in the United States the incidence is around 500,000. Most of those skin cancer cases are attributed to solar irradiance of the skin (UNEP, 1991). Previous attempts to estimate risks of ozone depletion have focused mainly on aspects of the source-effect chain (EPA, 1988; Kelfkens et al., 1990; De Gruijl, 1982; Moan, 1991; UNEP, 1991) and do not take into account all delay mechanisms involved: on the one hand between production, emission, atmospheric dispersion and ozone depletion and on the other between increased UV exposure and skin cancer incidence. The source-effect model developed in this study (Chapter 2) attempts to provide a state-of-the-art evaluation of the full source-effect chain.

Results obtained in applying the model are provided in Chapter 3. Three scenarios have been developed describing future production of CFC's (section 3.1). For each of these scenarios the CFC emission (section 3.1), atmospheric concentration of CFC's (section 3.2), stratospheric chlorine levels and ozone depletion (section 3.2) are estimated. The expected change in UV exposure of the biosphere is quantified (section 3.3). Excess incidence and mortality due to depletion of the ozone layer in the Netherlands are estimated in section 3.4. The results obtained and model uncertainties are summarised and discussed in Chapter 4. Possible impacts of an enhanced depletion, as expected by NASA in February 1992, are discussed in section 4.3. Conclusions of the study are presented in Chapter 5.

2 MODELLING THE SOURCE-EFFECT CHAIN

Environmental pollution can lead to negative side effects for human health and the environment. A general concept for the cascade of events that can occur following the emission of pollutants to the environment is outlined in the source-effect chain. Human activities can lead to environmental emissions (the sources); the emissions can disperse to various environmental compartments (air, ground, water) and/or to the food chain (the dispersion). The concentration of pollutants in the various environmental compartments and food chain give rise to exposure of humans and ecosystems (exposure). The exposure can lead to adverse effects (effects), and thus to risks for humans and the environment. The source effect-chain can also be applied to possible depletion of the ozone layer, as outlined below:

Sources (section 2.1)
- emission of CFC's to the atmosphere decrease the atmospheric absorption of the solar UV, and thus can also be considered as an indirect source of UV.

Dispersion (section 2.2)
- CFC's emitted in the troposphere disperse to the stratosphere where photodissociation leads to increases in stratospheric chlorine levels, causing a decrease in stratospheric ozone. Ozone in the stratosphere is the main atmospheric absorber of biologically effective UV.

Exposure (section 2.3)
- Decrease in ozone leads to increased solar UV irradiance at ground level; the UV irradiance needs to be weighted according to its effectiveness to obtain biologically effective UV. Depending on behaviour and surface orientation a fraction of the available effective UV is received.

Effects (section 2.4)
- This report will focus on the carcinogenic effect of UV irradiance of the skin. However, the method can also be applied to other effects if enough information on the dose-time-effect relationship and on the effectiveness of different wavelengths is available.

The source-effect model developed consists of seven basic modules, each describing specific elements of the above mentioned source-effect chain. The modules are briefly indicated in Table 2.1 and are described in the subsequent paragraphs in this chapter.

2.1 Halocarbon production and emission

2.1.1 Historical trends in production and emissions

CFC's have, since 1930, been produced in small quantities. A great increase in production and applications has occurred since 1950. Following scientific concern about a possible depletion of the atmospheric ozone layer, a ban on non-essential CFC applications (use as aerosol propellants) was introduced, leading to a slight decrease (10-15%) in estimated global production in the period 1974-1978. After that CFC production was assumed to remain at a constant level until 1983. However, in 1983 it was realised that the 'steady state' in production figures was in fact caused by a balance between a decrease in aerosol applications, and the steady increase in non-aerosol applications. A future increase in CFC production was again expected and overall production has further increased since 1984 (see Fig. 2.1 (CMA, 1987 and 1988; GEMS, 1989)). Following the discovery of the Antarctic ozone hole in 1985,

a protocol was developed aiming at a reduction of future CFC production (Montreal Protocol). The Montreal Protocol was followed by a more rigorous limitation of production in the London Amendments. Details on various production scenarios are provided in section 3.1.

TABLE 2.1 Source-effect chain for ozone depletion; outline of basic modules in the chain model

SOURCE-EFFECT CHAIN		UV OZONE CHAIN MODEL (section)	
SOURCES		Halocarbon production and emission (2.1)	Halocarbon production module (2.1.2)
			Halocarbon emission module (2.1.3)
ENVIRONMENTAL DISPERSION		Atmospheric dispersion and chemistry (2.2)	Halocarbon concentration module (2.2.2)
			Chlorine/bromine concentration module (2.2.3)
			Ozone depletion module (2.2.4)
EXPOSURE		Modelling atmospheric UV transfer (2.3)	Effective UV irradiance module (2.3.2)
EFFECTS		Dose-effect relationship for skin cancer incidence (2.4)	Dose-effect module (2.4.3)

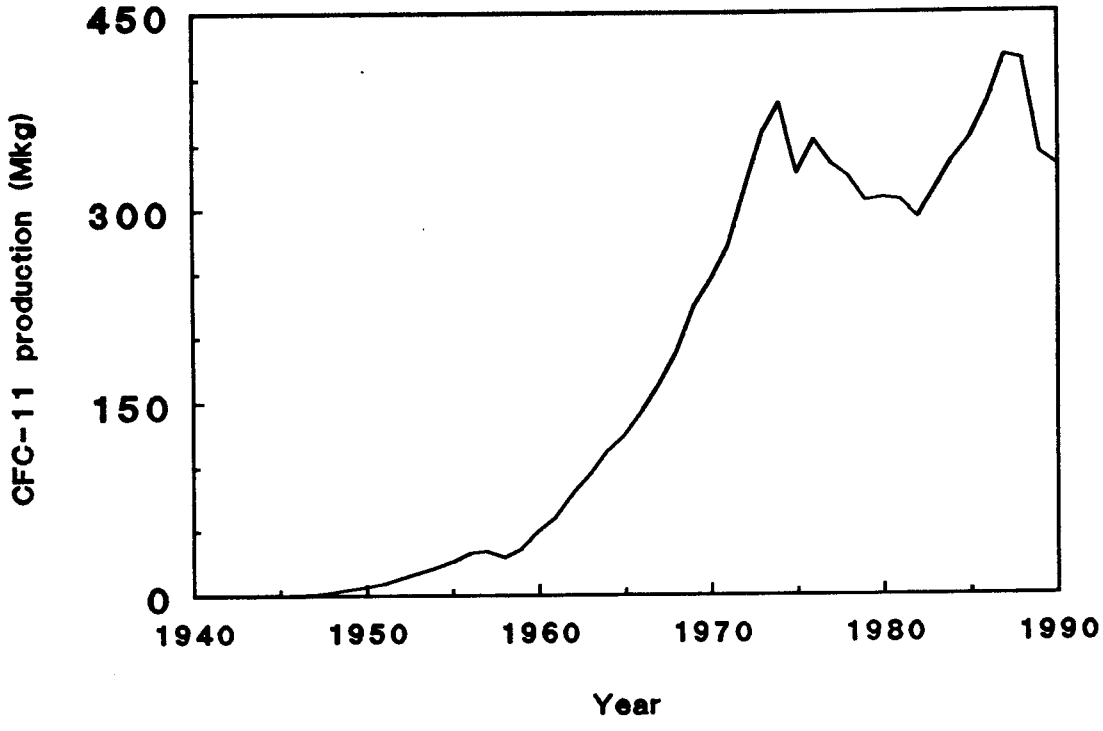

FIG. 2.1 Global production of CFC-11 from 1940-1990.

2.1.2 Halocarbon production module

This module provides the basic input for the emission module in the chain model: the production of halocarbons for five different application (end-use) categories are determined for three scenarios.

The halocarbon production module includes the following halocarbons, as described in Den Elzen et al. (1990) and Den Elzen et al. (1992):

- all currently regulated chlorofluorocarbons: CFC-11, CFC-12, CFC-113, CFC-114 and CFC-115;
- substitutes with lower ozone depleting potential: HCFC's (HCFC-22, HCFC-123, HCFC-124, HCFC-141b, HCFC-142b) and four HFC's (HFC-134a, HFC-125, HFC-143a, HFC-152a);
- other halogenated chemicals: methyl chloroform and carbon tetrachloride.

Five different major end-use categories for the chlorofluorocarbons and their substitutes are distinguished, each represented by a specific lifetime: aerosols, open cell foams and solvents (lifetime: less than one year), closed cell foams and non-hermetically sealed (four years) and hermetically sealed refrigeration (12 years) (Gamlen et al., 1986). Methyl chloroform and carbon tetrachloride are used mostly as solvents, implying there is hardly any delay between production and release (less than one year).

Historical data on production up to 1990 are used for the model (see Fig. 2.1 and section 2.1.1). Three different production scenarios are developed for the period after 1990. Production scenarios for developing and developed countries are distinguished (see section

3.1 for the production scenarios). Reduction of the regulated chlorofluorocarbon production is guided by three mechanisms:

- conservation and recycling: including recovery and better operating practices for these chlorofluorocarbons;
- substitution schemes by non-fluorocarbons;
- substitution by HCFC's/HFC's;

Future pathways for these reduction schemes are also specified in the assumptions of the emission scenarios.

2.1.3 Halocarbon emission module

The emission module calculates the atmospheric release of halocarbons. It is modelled using an emission box and a delayed-release box according to Wigley (1988), as described in Den Elzen et al. (1990). The total emissions of the halocarbons are split up into direct emissions, (released from the emission box) and indirect emissions, (released from the delayed-release box). The direct (first-year) emissions are composed of fugitive emissions and a first-year emission for each of the end-use categories, which is related to the inverse of the lifetime of the application. Besides these first-year emissions of the halocarbons the model also covers delayed-emissions. All halocarbons not released in the first year enter the delayed emission box. The delayed emissions are modelled as a fraction of the total halocarbon production stored in this box.

For each of the halocarbons under consideration the total emission is calculated by means of:

$$E_T(t) = \sum_A (P(A,t)\ (f_{fug} + \frac{1}{L_A})) + \beta E_D(t) \qquad (2.1)$$

where

$E_T(t)$ - total emission in year t, including direct emissions and indirect emissions from the delayed-emission box (Mkg/yr)

Σ - summation over all application categories A

$P(A,t)$ - production of a halocarbon compound used in a product of application category A in year t (result from module described in 2.1.2)(Mkg/yr)

f_{fug} - fraction of emitted halocarbons due to production losses (2% for CFC-11, 3.3% for CFC-12, 0 for other halocarbons (Den Elzen et.al., 1990)

L_A - lifetime of application A, $1/L_A$ represents emissions in the first year following production

$E_D(t)$ - total content of the delayed-release box for the compound under consideration (Mkg); calculated by means of equation (2.2).

β - fraction emitted per year from the delayed-release box.

The content of the delayed release box is calculated solving the following differential equation numerically:

$$\frac{dE_D(t)}{dt} = \sum_A (P(A,t)\ (1 - \frac{1}{L_A})) - \beta E_D(t) \qquad (2.2)$$

where the symbols are as provided above.

The summation over all end-use categories provides the total amount entering the delayed-release box: the total production not released during the first year. The second term in equation 2.2 denotes the loss from the delayed-release box. The constant β is fitted to obtain the best agreement with measurements of halocarbon concentration.

2.2 Atmospheric dispersion and chemistry

2.2.1 Introduction

In 1973 Lovelock found that CFC's were not destroyed in the lower atmosphere (troposphere). Instead it was shown that they accumulated in the lower atmosphere, and that concentrations increased over time. Molina and Rowland (1974) made the fact that small fractions of the CFC's are transported to the stratosphere plausible; here photodissociation by high-energy radiation occurs, thus leading to a release of chlorine, which could enter a catalytic cycle that would destroy ozone molecules. Since most of the atmospheric ozone is found in the stratosphere, the release of chlorine there could seriously reduce the total column ozone in the atmosphere. Since these first findings more than a hundred chemical reactions, which influence the complex chemical balance in the stratosphere, have been identified.

We have implemented a simple representation of the complicated atmospheric chemistry. Starting from the emissions tropospheric concentrations of halocarbons in line with present observations on historical trends, are calculated (section 2.2.2). Stratospheric concentrations are directly linked to tropospheric concentration and lead to the release of chlorine (and bromine). The chlorine and bromine module is outlined in section 2.2.3. Depletion of the ozone layer is linked to chlorine concentrations (see section 2.2.4).

2.2.2 Halocarbon concentration module

The tropospheric halocarbon concentrations are calculated using the total emission as calculated in the halocarbon emission module (section 2.1.3). The concentration module is directly linked to the emission box and the delayed-release box. The removal process of the chlorofluorocarbons and their alternatives is assumed to be inversely proportional to the atmospheric lifetimes of the halocarbons, the latter being constant as based on IPCC (1990), and Prather and Watson (1989). The troposheric concentration of CFC's is determined by the initial concentration, the emissions and their removal. CFC's are assumed to be removed from the atmosphere due to stratospheric loss only and in proportion to their concentration. The fraction of CFC's remaining at time t is reflected by the negative exponential function $e^{-t/L}$, where L is the atmospheric lifetime of the CFC concerned. The global tropospheric concentration used in the model is found solving:

$$\frac{dC_T(t)}{dt} = k_C E_T(t) - \frac{C_T(t)}{L_{CFC}} \qquad (2.3)$$

where

$C_T(t)$ - tropospheric concentration of a halocarbon in year t (pptv)
k_C - conversion factor, from emission to concentration (pptv/Mkg)
$E_T(t)$ - total emission calculated in section 2.1.3 (Mkg/yr)
L_{CFC} - atmospheric lifetime of CFC.

The concentrations of all halocarbons are modelled in analogous fashion.

2.2.3 Chlorine/bromine concentration module

Atmospheric chlorine concentrations are steadily increasing at a rate of 3% per year. The chlorine loading in the stratosphere has gone up from 2 ppbv in the late 1970s to present values of about 3.5 ppbv. This is a factor of 5 to 6 above the estimated natural level of 0.6 ppbv, originating from methyl chloride (WMO/UNEP, 1989). In this module we use a linear relationship between the concentration of halocarbons and the concentration of released chlorine in the stratosphere (EPA, 1988):

$$Cl(t) = Cl(0) + \sum_{CFCs,HCFCs,HFCs,CCl_4,CH_3CCl_3} k_{CL}.[C_T(t-4)] \qquad (2.4)$$

where

Cl(t) - chlorine level at time t (ppbv)
Cl(0) - background chlorine level (0.6 ppbv)
Σ - summation over all halocarbons
k_{CL} - chlorine conversion factor of halocarbon under consideration (ppbv of chlorine per pptv of tropospheric halocarbon concentration)
$C_T(t-4)$- tropospheric concentration of halocarbon under consideration four years prior to the year t (see text below) (pptv).

Because it takes on average two years for the halocarbons to diffuse from the troposphere to the stratosphere, and typically another two years to photolyse halocarbons at a 20-km height, there is a delay of four years in the coupling between the tropospheric halocarbon concentration and stratospheric chlorine (see equation 2.4).

2.2.4 Ozone depletion module

This module calculates yearly averaged ozone depletion in relation to the chlorine concentrations.

Because stratospheric ozone depletion is a not yet a fully understood result of transport, radiation and perturbed chemistry, any simple analytic description is necessarily a crude one. Most catalytic ozone destruction cycles are known (NO, OH, ClO, BrO), but their importance for ozone destruction in the lower stratosphere remains a puzzle due to the many confounding factors like temperature, radiation balance, stratospheric clouds and aerosols originating from vulcanos (e.g. Pinatubo).

Nevertheless, it has become clear from laboratory studies, fieldwork and satellite measurements that ozone depletion is strongly coupled to the chlorine loading in the atmosphere. Independent of the exact mechanisms we have therefore used a linear relationship between yearly averaged ozone depletion and stratospheric chlorine concentration:

$$(\Delta O(t)/O) = k\,(Cl(t)-Cl(0)) \qquad \textbf{(2.5)}$$

where

$\Delta O(t)/O$- yearly averaged relative decrease in total column ozone (per cent %)

k - constant relating chlorine concentration to ozone depletion (per cent depletion per ppbv chlorine; see Table 2.2)

Cl(t) - yearly averaged stratospheric chlorine concentration in ppbv

Cl(0) - background concentration of chlorine at which no depletion of the ozone layer is assumed to occur (0.6 ppbv for model evaluations; 2 ppbv for TOMS-based evaluations).

The values for the no-effect level (Cl(0)) and the scaling factor (k) in equation (2.5) are derived from:

- model calculations from (WMO/UNEP, 1989 (further referred to as model-based estimates), and
- satellite-based measurements of total column ozone depletion (further referred to as TOMS-based estimates) from Stolarski et al. (1991).

The WMO/UNEP (1989) calculations through various 1D and 2D global dispersion models of the stratosphere take the methyl chloride concentration of 0.6 ppbv Cl as zero level. The ozone depletion predicted by the models for a number of CFC scenario studies shows large scatter. The scaling factor k, derived from these model results, is given in Table 2.2 for two latitudes.

The total ozone observations, taken over the period 1979-1990 by the TOMS instrument, indicate that ozone depletion occurs much more rapidly than predicted by the above-mentioned models (Stolarski et al., 1991). From these observations we have derived a relationship between ozone depletion and chlorine concentrations that tends to increase by 1 ppbv Cl per decade (Table 2.2). Note that the TOMS observations show a very pronounced seasonal variation in ozone depletion, that will be described below (see section 2.3.2, Fig.2.3). Contrary to the model assumptions we have taken an empirical no-effect level of 2.0 ppbv Cl, because:

- the ozone hole above the Antarctic, where the atmospheric influence of Cl is magnified as compared to the Northern Hemisphere, started to appear after 1975 when the Cl level was 2.0 ppbv;
- backward extrapolation of the TOMS (1979-1990) relationship would lead to total ozone depletion of more than 10% at mid-latitudes, which is contradicted by the ground-based ozone observations from the Dobson network.

TABLE 2.2 Values of parameter k for 50 and 40° Northern Latitude (NL)		
Basis for k estimates	50 NL	40 NL
WMO model-calculations	1.11 ± 0.30 % per ppbv	1.00 ± 0.25 % per ppbv
TOMS measurements	4.9 % per ppbv	4.3 % per ppbv

2.3 Modelling atmospheric UV transfer

2.3.1 Introduction

The solar UV spectrum is strongly influenced by atmospheric absorption and scattering. Ozone is the primary absorber of the UV-B, and molecules and aerosols are the primary scatterers. Spectral UV irradiances at the earth's surface were calculated for various solar altitudes and various thicknesses of the ozone layer. Spectral irradiances were obtained at sea level, using a previously developed atmospheric UV transfer-model (De Leeuw, 1988). In this model the radiative transport through the atmosphere, as a series of layers, was calculated numerically. In each layer absorption and scattering were taken into account in a linear approximation. An urban aerosol profile and a standard ozone profile were used in the calculations. Direct and diffuse radiation were considered separately. The model has been validated against available incidental measurements of UV (De Leeuw and Slaper, 1989). The measurements of trends in UV irradiance are lacking at present. On the basis of model results we obtained simple analytical expressions describing the relationship between UV irradiance and thickness of the ozone layer as a function of season and latitude. The methods used are outlined in section 2.3.2; the simplified relationships obtained using the detailed UV transfer-model, were implemented in the dose-effect module (section 2.4).

2.3.2 Determination of effective UV irradiance

The monthly total effective UV-dose was calculated for two latitudes and various thicknesses of the ozone layer. Applying the previously developed UV transfer model (De Leeuw, 1988), monthly time integrated spectral irradiances were calculated. The monthly total spectral irradiance was then weighted with an action spectrum to obtain an effective monthly dose:

$$D_i(O) = \Sigma\, S_i(O,\lambda)\, A(\lambda) \qquad \textbf{(2.6)}$$

where

- Σ - sum over UV wavelength range of 100 to 400 nm; the sum is taken for nanometer intervals as a numerical approximation of an integration over the UV range
- $D_i(O)$ - effective dose on horizontal plane for month i and for ozone thickness O (mJ/cm^2)
- $S_i(O,\lambda)$ - monthly total spectral dose for month i and at wavelength λ; S is given in $mJ/(cm^2\ nm)$
- $A(\lambda)$ - relative effectiveness at wavelength λ (action spectrum).

The action spectrum used was previously determined as an action spectrum for

photocarcinogenesis in the hairless mouse (Slaper, 1987; UNEP, 1989). Fig. 2.2 provides the action spectrum used. Effective UV doses were calculated for each month of the year (see Fig. 2.3).

We determined the effective dose for each month in relationship to the thickness of the ozone column. The thickness of the ozone column was varied from 220 to 380 Dobson Unites (DU; 300 DU correspond to a thickness of the ozone layer of 0.3 cm at standard temperature and presssure).

For each latitude under consideration and for each month a fourth order polynomial was fitted to describe the relationship between effective doses and ozone thicknesses.

The polynomial approximations were used as the functional relationship between effective UV dose and thickness of the ozone layer. The calculation of the yearly total effective dose is a straightforward summing of the monthly totals, taking two complications into account:
- there is a natural variation of the thickness of the ozone layer,
- depletion of the ozone layer is expected to vary within a year (see Fig. 2.3)

The thickness of the ozone layer shows a natural seasonal variation that (at 52 NL) can be approximated by a sinusoidal variation with a maximum in the spring (Bowman, 1985).

$$O_i = O + O_A \cos((2\pi/12)(i - \phi)) \qquad \textbf{(2.7)}$$

where

O_i - thickness of the ozone layer at month i (DU)

O - reference value of yearly averaged thickness of the ozone layer at the latitude under consideration (DU): 330 DU for 52° NL)

O_A - amplitude describing yearly variation of thickness of the ozone layer (50 DU for 52° NL)

ϕ - phase shift, four months: the maximum thickness of the ozone layer in April (month 4) is 380 DU.

Equation (2.7) applies when the ozone layer is not depleted. If the yearly averaged depletion is given by ΔO, then for each month in the year the relative depletion is given by:

$$(\Delta O_i/O_i) = c_i (\Delta O/O) \qquad \textbf{(2.8)}$$

where

ΔO_i - depletion of ozone layer in month i (DU)

c_i - a series of correction factors, obtained by dividing the relative depletion in month i by the yearly averaged relative depletion (see Fig. 2.3)

The annual dose of effective UV can then be calculated applying the previous equations and summing the effective UV dose in each month:

$$D(O- \Delta O) = \Sigma D_i(O_i- \Delta O_i). \qquad \textbf{(2.9)}$$

Using equation (2.9) the yearly total effective UV dose was calculated for various thicknesses

of the ozone layer. The calculated data points were interpolated using a fourth-order polynomial fitted to the data points.

$$D(O\text{-}\Delta O(t)) = a_0 + a_1 (\Delta O(t)/O) + a_2 (\Delta O(t)/O)^2 + a_3 (\Delta O(t)/O)^3 + a_4 (\Delta O(t)/O)^4 \quad \textbf{(2.10)}$$

where

$a_0..a_4$ polynomial coefficients (in mJ/cm^2; Table 2.3 provides the values when $\Delta O(t)/O$ is expressed as a percentage decrease).

$D(O\text{-}\Delta O(t))$ effective UV dose (mJ/cm^2)

The difference in the polynomial coefficients for TOMS and model evaluations is caused by the differences in the seasonal variation of ozone depletion (Fig. 2.3).

TABLE 2.3 Polynomial coefficients for 52 and 40° NL

Latitude	52 NL		40 NL	
Parameter	Model (mJ/cm^2)	TOMS (mJ/cm^2)	Model (mJ/cm^2)	TOMS (mJ/cm^2)
a_0	51,557	51,557	77,432	77432
a_1	743.5	662.2	1154	962.3
a_2	9.549	10.25	14.66	14.31
a_3	0.05765	0.039	0.1107	0.09652
a_4	0.001859	0.005696	0.002443	0.007583

2.4 Dose-effect module for skin cancer incidence

2.4.1 Scientific basis

The first suggestions that skin cancer could be caused by repeated exposure to sunlight were given at the end of the last century. Since then much information from clinical, epidemiological and experimental studies has been gained. When discussing the relationship between UV exposure and skin cancer incidence one should differentiate between non-melanoma skin cancer and melanoma skin cancer.

The most common type is non-melanoma skin cancer (90% of total). Lethality is usually less than 1%. Non-melanomas are subdivided into basal cell carcinoma and squamous cell carcinoma. UV exposure is generally considered as the major cause for the occurrence of non-melanoma skin cancers (UNEP, 1989). See section 2.4.2 for incidence and mortality estimates.

Melanoma skin cancers are less common, but lethality of these cancers is high (25%). The relationship between UV exposure and melanoma incidence is not very clear. The general impression is that UV exposure contributes to the incidence of melanoma, but the extent is not well understood. The incidence of melanoma has been shown to have risen rapidly (5-7% per year) over the past 3 to 4 decades.

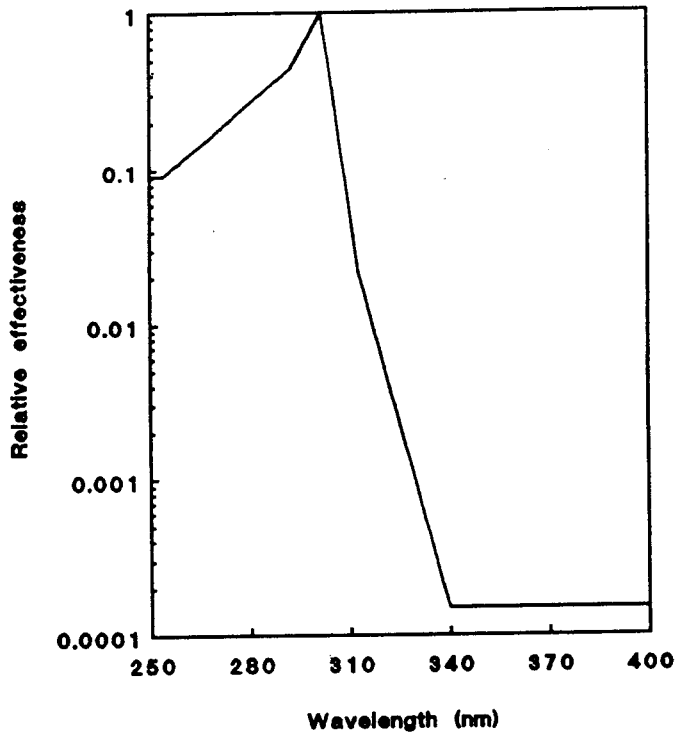

FIG. 2.2 Action spectrum for UV photocarcinogenis in the hairless mouse.

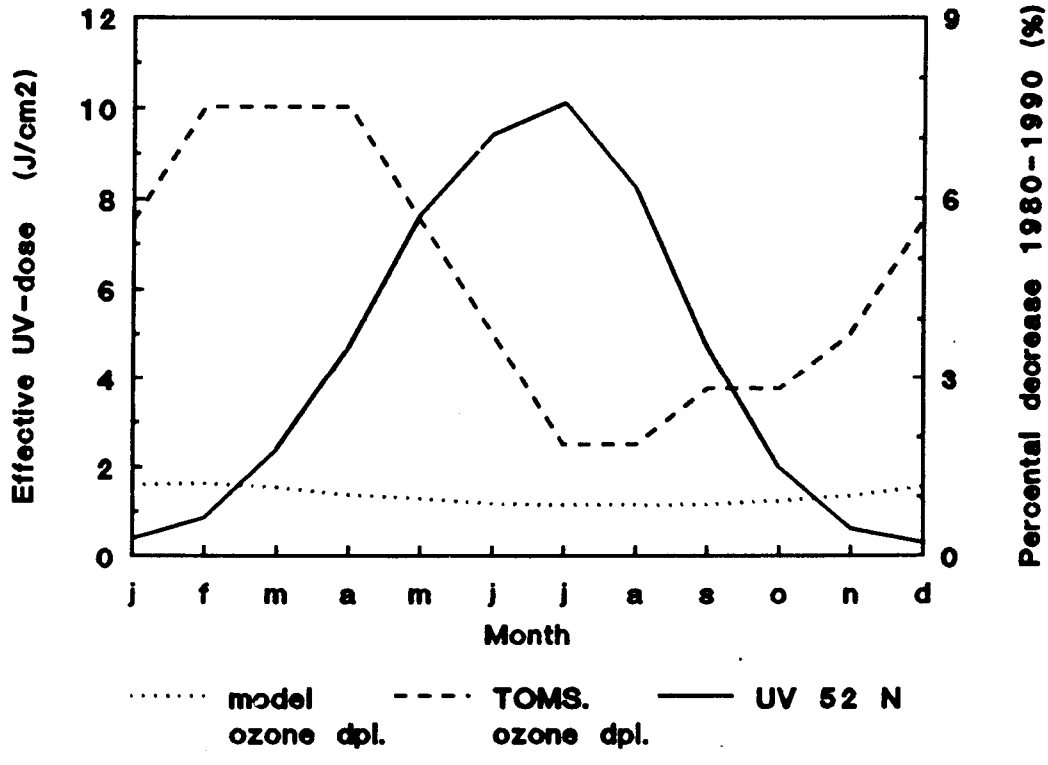

FIG. 2.3 Seasonal variation in effective monthly UV dose in the Netherlands and in ozone depletion according to TOMS- and model-based estimates.

A brief summary of evidence in support of the causal role of UV exposure follows:

- the incidences of both non-melanoma and melanoma skin cancer are higher at lower geographical latitudes, where the solar UV irradiance is higher;
- incidence of non-melanoma skin cancer is higher among people with outdoor professions (i.e. this does not apply to melanoma incidence);
- non-melanoma skin cancers occur primarily on the most exposed skin sites (approximately 80% occur on the head and hands; for melanoma 20-25% occur on the head and hands);
- non-melanoma and melanoma incidences are higher in Caucasians, and especially among the groups with a sunburn sensitive skin;
- incidences are higher among people who suffer from genetic disorders which lead to increased sensitivity to the sun (xeroderma pigmentosum, albinism);
- UV radiation induces skin cancer in animals (extensive dose-response studies have shown clear relationships between UV exposure and the induction of squamous cell carcinoma in mice (and rats). Recently, two animal models have been found for melanomas);
- UV radiation induces damage and mutations in cellular DNA and can cause cell death.

In order to provide quantitative estimates of the skin cancer incidence in relation to ozone depletion information is needed on:

- the relation between doses received and incidences, i.e. dose-response information;
- the relative effectiveness (effective weighting factor) of various wavelengths, often summarised in terms of an action spectrum.

Information on the dose-response relationship can be obtained from animal experiments and from epidemiological data from various latitudes. Using functional relationships derived from animal dose-response studies the model parameters can be adjusted on the basis of the epidemiological data from various latitudes, provided that knowledge of the action spectrum is available. The latter is necessary since the solar spectrum varies with the solar altitude and thus with the time of day, time of year and latitude. An action spectrum for photocarcinogenesis for humans is not available. Therefore we used an action spectrum derived from experimentation in hairless mice (UNEP, 1989; Slaper, 1987; Sterenborg, 1987). This action spectrum shows a rough similarity to the action spectum for erythema in human skin (Parrish et al., 1982). It should be noted that the results in animal studies apply to squamous cell carcinoma. We used similar functional relationships and action spectra for a quantitative evaluation of basal cell carcinoma and melanoma. The parameters in the relationship have been fitted to available epidemiological data on each type of skin cancer separately.

The cumulative number of skin cancer cases upto age a (the cumulative incidence Y(a)) is calculated using (Slaper et al., 1986):

$$Y(a) = \gamma \, (\Sigma_{j=1..a} E(j))^c \, a^{d-c} \qquad \textbf{(2.11)}$$

where

a	- age a (years)
$\Sigma_{j=1..a} E(j)$	- cumulative effective UV dose received by the skin upto age a
E(j)	- effective UV dose received in the year at age j (mJ/cm^2)

γ - model parameter depending on the type of skin cancer, the sensitivity of the population, and the skin area exposed

c, d - model parameters describing dose- and time dependence of the incidence.

The parameters c and d are specific for the type of skin cancer. The parameter c is often referred to in the literature as the biologic amplification factor: a 1 % increase in effective UV dose leads to a c % increase in incidence.

Table 2.4 gives the estimates for the various model parameters for basal and squamous cell carcinoma and for melanoma. We used epidemiological data for skin cancer incidence from the third national skin cancer survey in the USA (Scotto et al., 1981) in order to estimate the model parameters for basal cell and squamous cell carcinoma. The epidemiological data for age-specific incidences were used to estimate parameter d, and the incidence data for various latitudes were used to estimate the parameters c. For melanoma we used estimates derived from EPA, 1987. Estimating the parameter d for melanoma required a slightly different approach, since melanoma incidence rates are found to rise rapidly with new birth cohorts, thus it is not possible to use the age-specific incidence in a particular year. We therefore used age-specific incidences for three separate birth cohorts (derived from EPA, 1987). The values for the parameters γ are estimated on the basis of the present incidence.

TABLE 2.4 Parameter estimates used for evaluation of skin cancer risks

skin cancer type	c	d
melanoma	0.6	4.7
squamous cell carcinoma	2.5	5.7
basal cell carcinoma	1.5	4.9

2.4.2 Present mortality and incidence of skin cancer

The yearly mortality rate for non-melanoma skin cancer in the Netherlands is 80-90 (6 per million) persons (Gezondheidsraad, 1986). The present incidence of non-melanoma skin cancer is not very well-known in the Netherlands, due to the fact that registration is incomplete. On the basis of limited available statistics an incidence of 400-500 per million was estimated (Gezondheidsraad, 1986). It was indicated that this number should probably be regarded as an underestimate (Gezondheidsraad, 1986). A special skin cancer survey in the USA had shown that official registries were underestimating the total incidence numbers by a factor of 2.5 (Scotto et al., 1981). Assuming that the same applies to the situation in the Netherlands 1125 cases per million per year are estimated. Based on an extrapolation of the figures from the third national skin cancer survey in the USA and taking into account the lower solar intensity in the Netherlands, 1250 cases per million per year are estimated for the Netherlands. Neering and Cramer (1988) estimated the non-melanoma skin cancer incidence at 15,000 cases (1000 per million) per year.

In our calculations we used a present incidence of 15,000 basal cell carcinomas (1000 per million) per year, and 1500 squamous cell carcinoma (100 per million) per year. Lethality

percentages are estimated to be 0.3% for basal cell carcinoma, and 3% for squamous cell carcinoma. These figures are in line with the above mentioned mortality rate of 6 per million per year.

The present estimate of the yearly mortality rate for melanoma in the Netherlands is approximately 300 (20 per million persons per year (based on Gezondheidsraad, 1986). The yearly incidence is estimated to be 1200 (80 per million per year).

2.4.3 Dose-effect module

The effective dose received by the skin is a fraction of the available solar effective UV dose. The fraction received depends on the behaviour with respect to UV exposure and the available dose, which depends on the ozone content in the year under consideration. We assumed that the total effective UV exposure is due to solar exposure, and that the effective UV dose received by the skin of people who are of age a in the year T is given by:

$$E(a,T) = \beta(a)\ D(O(T)) \qquad \textbf{(2.12)}$$

where $\beta(a)$ represents the exposure fraction received by the most exposed parts of the skin (head and hands). In our calculations we assumed $\beta(a)$ to be independent of the age a, and a value of 0.02 was taken. D(O(T)) was calculated according to the UV transfer model described above. The UV transfer model provides estimates for cloudless conditions, and thus must be seen as an overestimation of the yearly dose on a horizontal plain. Including the effects of average cloud cover, the dose is expected to be reduced to 65%. Thus the exposure percentage of 2% corresponds to an exposure percentage of 3% under average cloud conditions, which corresponds to an average exposure for indoor workers in the Netherlands (Slaper, 1987). It should be noted that other values for $\beta(a)$ do not influence the results of our estimates, if, as we assumed, the exposure fraction does not change over time, and/or with age. Changes in the value of $\beta(a)$ lead to changes in the estimated parameter γ (equation 2.11), but not to the number of additional cases of skin cancer.

The exposure received by the skin changes over the years due to the change in the ozone column, and therefore applying equation 2.11, we can state:

$$Y(a,T) = \gamma\ (\Sigma_{j=1..a}\ E(j,T-a+j))^c\ a^{d-c} \qquad \textbf{(2.13)}$$

where

Y(a,T)	-	cumulative incidence in group with age a in year T (cases per million)
a	-	age (year)
E(j,T-a+j)	-	exposure at age j for a person who has age a in year T (mJ/cm^2)
$\Sigma_{j=1..a}\ E(j,T-a+j)$	-	cumulative effective UV dose received by the skin upto age a (mJ/cm^2)
E(j)	-	effective UV dose received in the year at age j (mJ/cm^2).

The age-specific incidence (I(a,T)) at age a in the year T is calculated using:

$$I(a,T) = (Y(a+1,T+1)-Y(a,T)) \qquad \textbf{(2.14)}$$

The yearly incidence within the total population can be calculated by means of:

$$I(T) = \Sigma\, N(a,T)\, I(a,T) \qquad \textbf{(2.15)}$$

where
Σ - sum over all age groups
N(a) - the number of people in age group a.

3 RESULTS

3.1 CFC production scenarios

In this study we use the historical data on production until 1990. For the period 1990-2100 three scenarios were used. The assumptions of the three scenarios are summarised in Table 3.1. All scenarios considered assume a global reduction in CFC production, along the lines of international protocols. Of the scenarios considered, the Montreal Protocol is associated with the highest production levels. The second scenario implies a partial implementation of the London Amendments to the Montreal protocol, assuming that 70% of the developing world is fully complying. The last scenario is a full implementation of the London Amendments.

Table 3.1 Production scenarios for halocarbons

halocarbons	CFC's, methyl chloroform and carbon tetrachloride	HCFC's and HFC's
Montreal Protocol scenario	Production of five regulated CFC's decrease according the Montreal Protocol to 20% in 1993 and 50% in 1998 for the developed countries and for the developing world 10 years later. The production of methyl chloroform and carbon tetrachloride remain at the 1990 level.	Alternatives (HCFC's and HFC's) replace 35% of the phased-out CFC's and increase by 2.5% annually.
Partial London Amendments	Partial implementation of the London Amendments for the CFC's and other chemicals. 70% of the developing world is complying. In the non-participating countries the production of CFC's starts to increase during the next century (average yearly rate of 2.5% yearly).	Alternatives (HCFC's and HFC's) replace 35% of the phased-out CFC's and increase by 2.5% yearly.
London Amendments	Complete phase-out of CFC's by the year 2000 and methyl chloroform and carbon tetrachloride by 2010.	Alternatives (HCFC's and HFC's) replace 35% of the phased-out CFC's and increase by 2.5% yearly.

The production scenarios of CFC-11 are depicted in Fig. 3.1. Here we see that in the case of the Partial implementation of the London Amendments, the production of CFC's declines

rapidly till 2010, reflecting the phase-out of the countries complying with the provisions of the London Amendments. After 2010, the production of the CFC's starts to grow again due the countries not complying with the Protocol. The CFC-11 emission scenarios are depicted in Fig. 3.2.

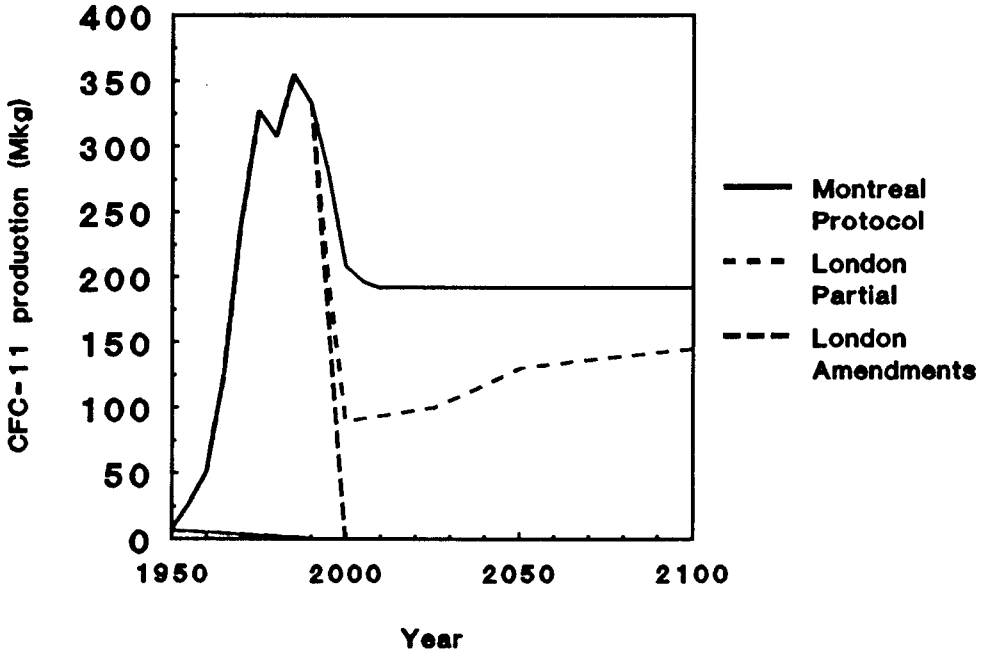

FIG. 3.1 Three future scenarios of the production of CFC-11. Only full compliance with the London amendments of the Montreal Protocol will ban this halocarbon.

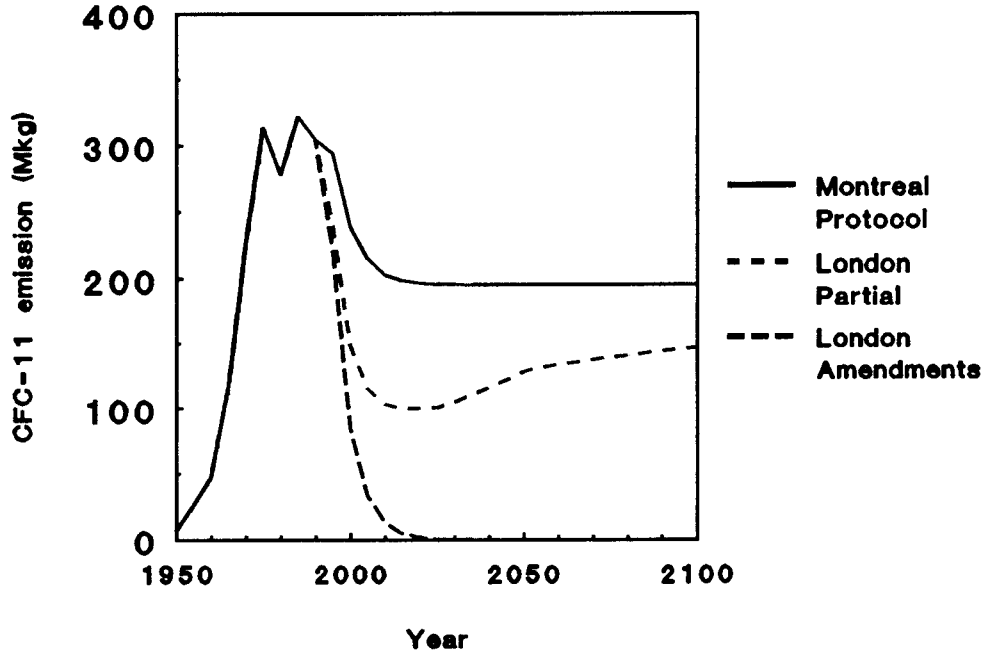

FIG. 3.2 CFC-11 emission scenarios.

3.2 Atmospheric dispersion and chemistry

The tropospheric concentrations of CFC-11 for the various scenarios are shown in Fig. 3.3. This figure shows the delay mechanism. Only for the London Amendments do the concentrations reach a level below that of 1990. For the three scenarios the chlorine levels are depicted in Fig. 3.4. For the Montreal Protocol the Cl concentrations increase constantly up to 6.9 ppbv in 2100. The same pattern can be seen for the partially implemented London Amendments, although the increase is less and leads to 4.7 ppbv in 2100. Global compliance to the London Amendments is expected to lead to maximum chlorine levels of 4 ppbv around the year 2000, declining to 2.4 ppbv in 2100.

The depletion of ozone due to increases in chlorine levels is estimated in two ways (see section 2.2.4):

- on the basis of detailed models of atmospheric chemistry (WMO/UNEP, 1989),
- on the basis of satellite measurements of total column ozone in the previous decade.

The results of both estimates are shown in Fig. 3.5 A (model-based) and 3.5 B (TOMS-based). The model-based estimates show approximately three-times lower depletions, as compared to the TOMS-based estimates: 4% average depletion is expected in the year 2000 according to the model based calculations, whereas 10% depletion is expected in the TOMS-based estimates. The model based estimates underestimate the ozone depletion observed at present, therefore the TOMS-based estimates are preferred.

3.3 UV transfer

The UV change associated with changes in thickness of the ozone layer is calculated for the various scenarios. Fig. 3.6 A provides the results based upon the model estimates of ozone depletion, assuming that there is no change in other parameters influencing UV transfer in the atmosphere. We also calculated the UV increase using the empirical approach based on TOMS satellite measurements of ozone depletion (results shown in Fig. 3.6 B).

3.4 Skin cancer incidence and death due to ozone depletion

We have evaluated the effects of ozone depletion on skin cancer incidence for the Netherlands (at 52 NL) and the USA (at 40NL).

A number of factors are expected to influence future skin cancer incidence:

- the age distribution of the population,
- the size of the population,
- (changing) exposure habits,
- sensitivity of the population,
- increases in effective UV irradiance, as caused by a depletion of the ozone layer.

It is not very likely that the sensitivity of the population is changing, and thus we have assumed that the sensitivity remains as it is. The age distribution and size of the population will certainly change over the years. We have evaluated the effects of these changes taking into account a population mid-scenario for the Netherlands (obtained from the Central Bureau of Statistics in the Netherlands). The results of these evaluations are presented in section 3.4.2. In order to separate the effects of ozone depletion from ageing effects in the population

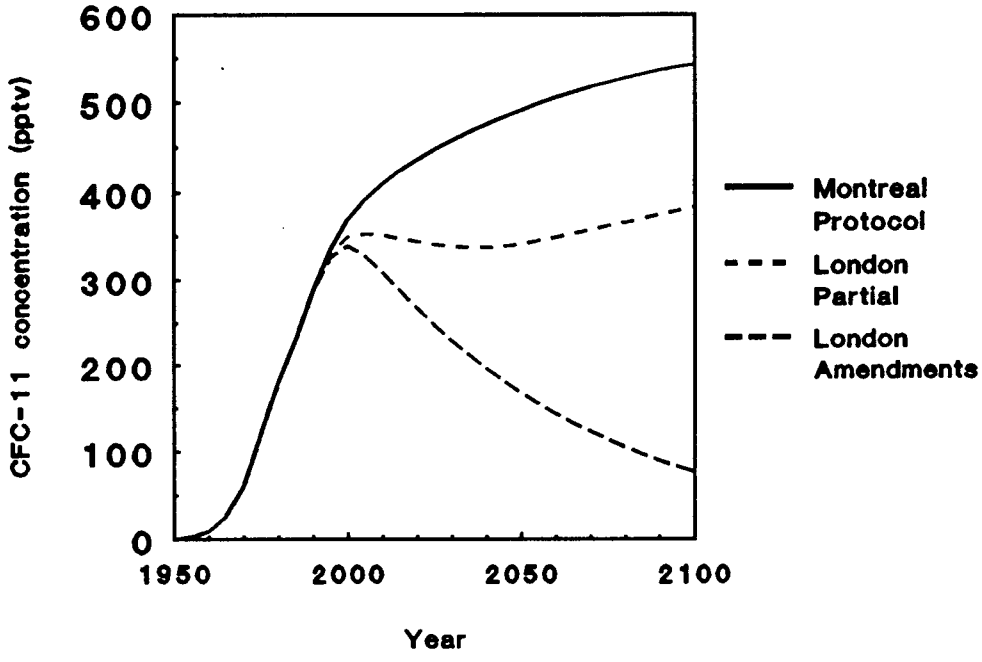

FIG. 3.3 Tropospheric CFC-11 concentrations.

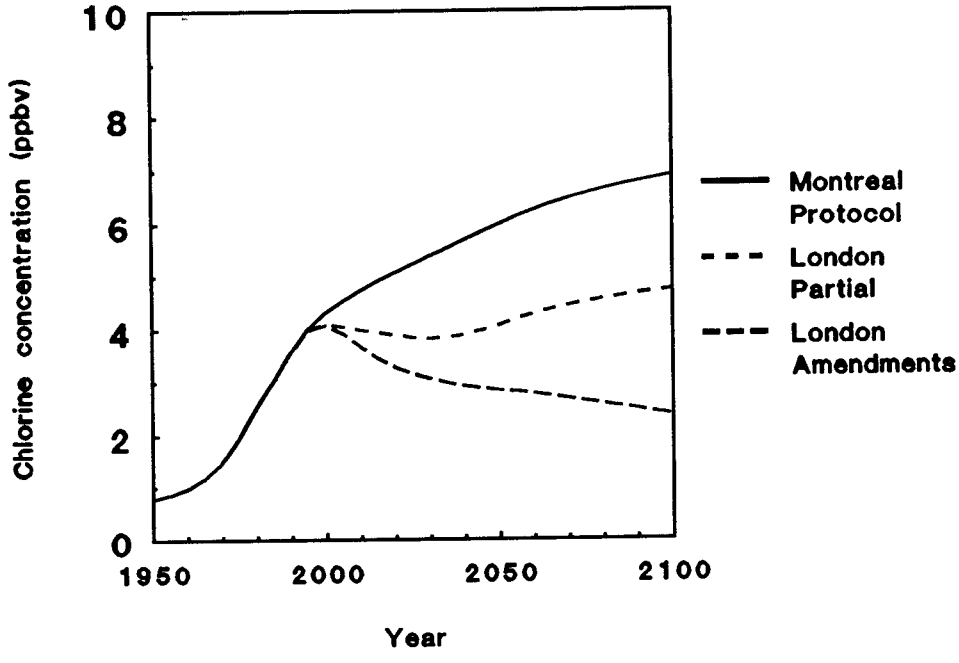

FIG. 3.4 Chlorine concentrations for three scenarios. The Cl loading will rise to more than 4.0 ppbv after the year 2000.

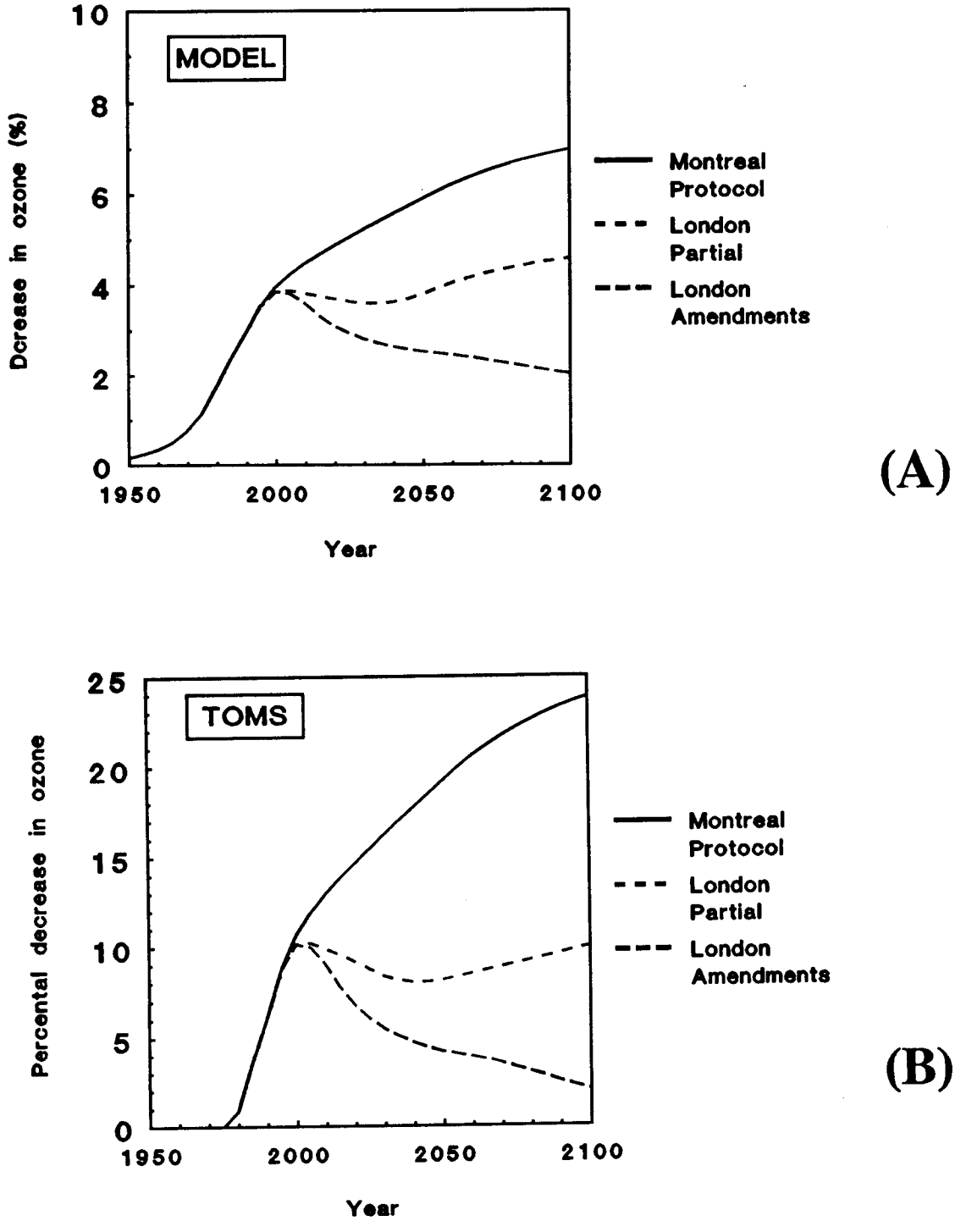

FIG. 3.5 Predicted evolution of the ozone layer above the Netherlands, as derived from WMO/UNEP models (A) and TOMS observations (B).

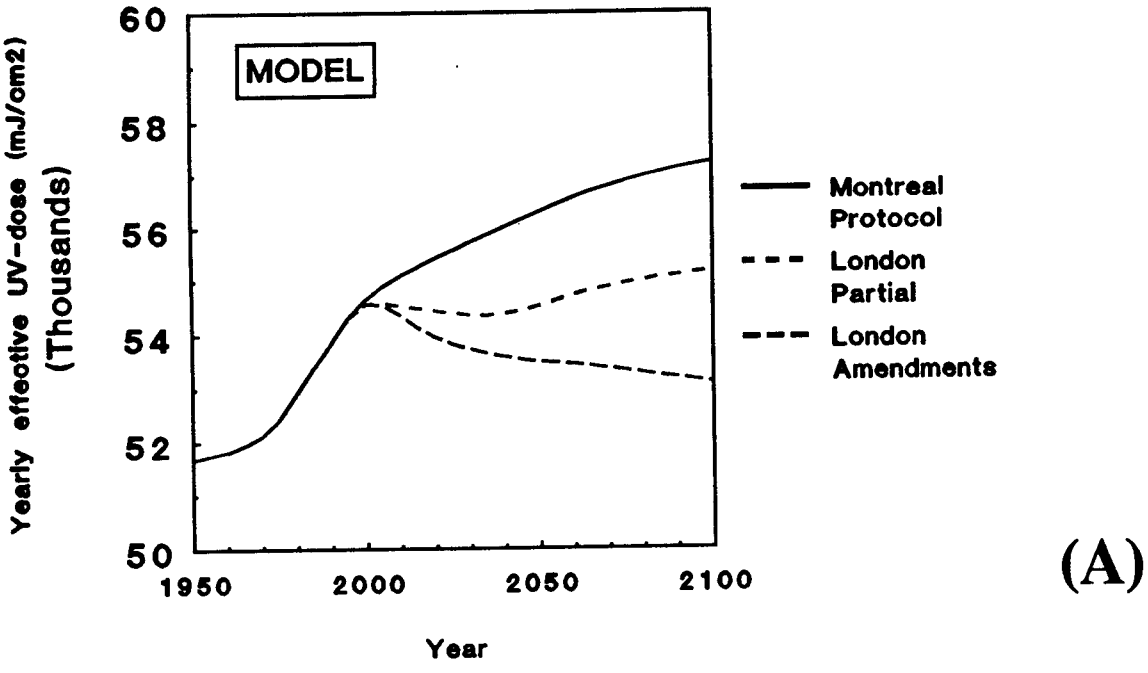

(A)

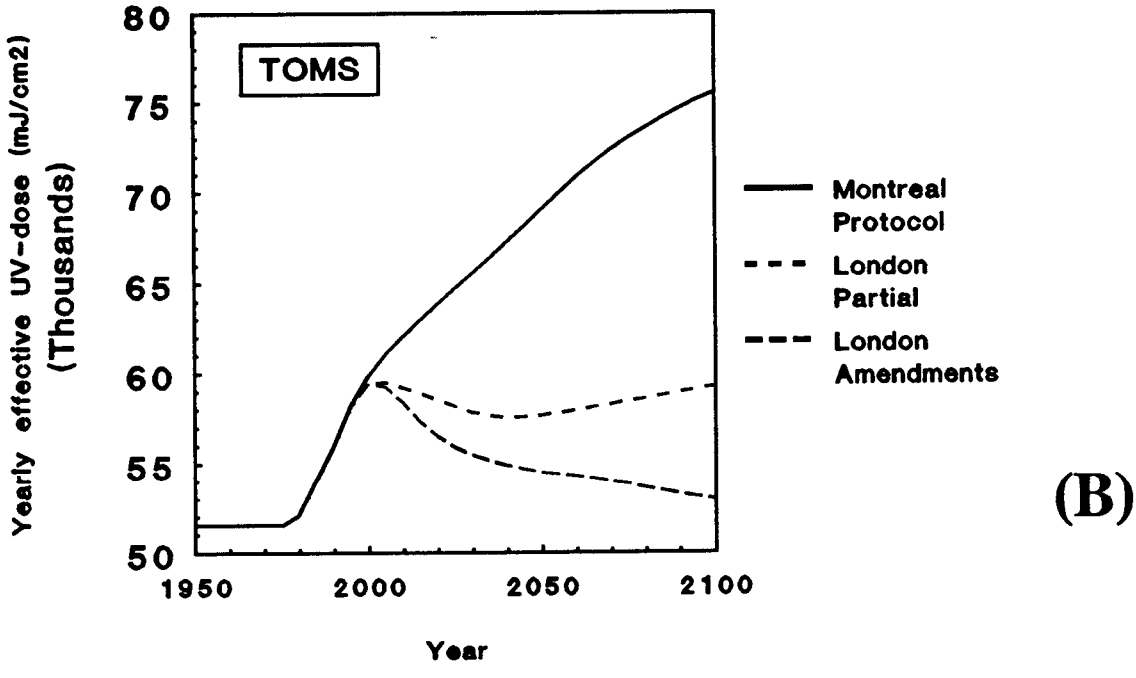

(B)

FIG. 3.6 Predicted increase in effective UV dose in the Netherlands (52 NL), as derived from WMO/UNEP models (A) and TOMS observations (B).

we have also performed calculations with a standardized population (the 1990 age-distribution in the Netherlands). Results are provided in section 3.4.1.

An estimation of future exposure habits is not included since it can be very dependent on trends. We assumed that exposure habits do not change over the evaluation period.

3.4.1 Excess rates of skin cancer incidence in the Netherlands (1990 population)

All results shown deal with excess rates, defined as the extra number of cases or deaths per year expected as a consequence of ozone depletion. All the results provided in this section are based on the age distribution of the 1990 population in the Netherlands.

Fig. 3.7 provides the estimated excess death rate due to skin cancer by summing, the excess death rates for melanoma and non-melanoma skin cancer. As indicated in section 3.4 modelling efforts of present ozone depletion underestimate the observed reduction in satellite (TOMS) measurements. We have therefore calculated the excess death rates for two situations: one in which the ozone depletion is estimated on the basis of models for atmospheric chemistry (Fig. 3.7 A) and one in which results of TOMS measurements are used for the estimation of future trends in ozone depletion (Fig. 3.7 B). The results show, that for the London Protocol a maximal excess death rate is expected to occur around the year 2050, with a slight decrease afterwards. The maximal excess rate is 2.2 per million per year for the TOMS-based estimates and 1.0 per million per year for the model-based evaluations. The excess death rates for the Montreal protocol continue to rise throughout the next century and for the year 2100 excess death rates of 10.6 per million per year for the TOMS-based and 2.4 per million for the model-based estimates are calculated.

We have also calculated the excess number of cases expected for melanoma and non-melanoma skin cancer. Fig. 3.8 provides the estimates for the excess number of melanoma and Fig. 3.9 gives the results for the excess number of non-melanoma skin cancer cases. Both figures show the TOMS-based estimates. For the London protocol a maximum excess incidence of 4.3 per million per year is calculated for melanoma and 161 per million per year for non-melanoma (maxima obtained in 2050). For the Montreal Protocol no maximum occurs over the calculated period, and the excess incidence rates in the year 2100 are 18.5 per million per year for melanoma and 801 per million per year for non-melanoma. The estimated excess rates for the London Protocol are in the year 2100 at least eight times lower than the estimated rates for the Montreal Protocol.

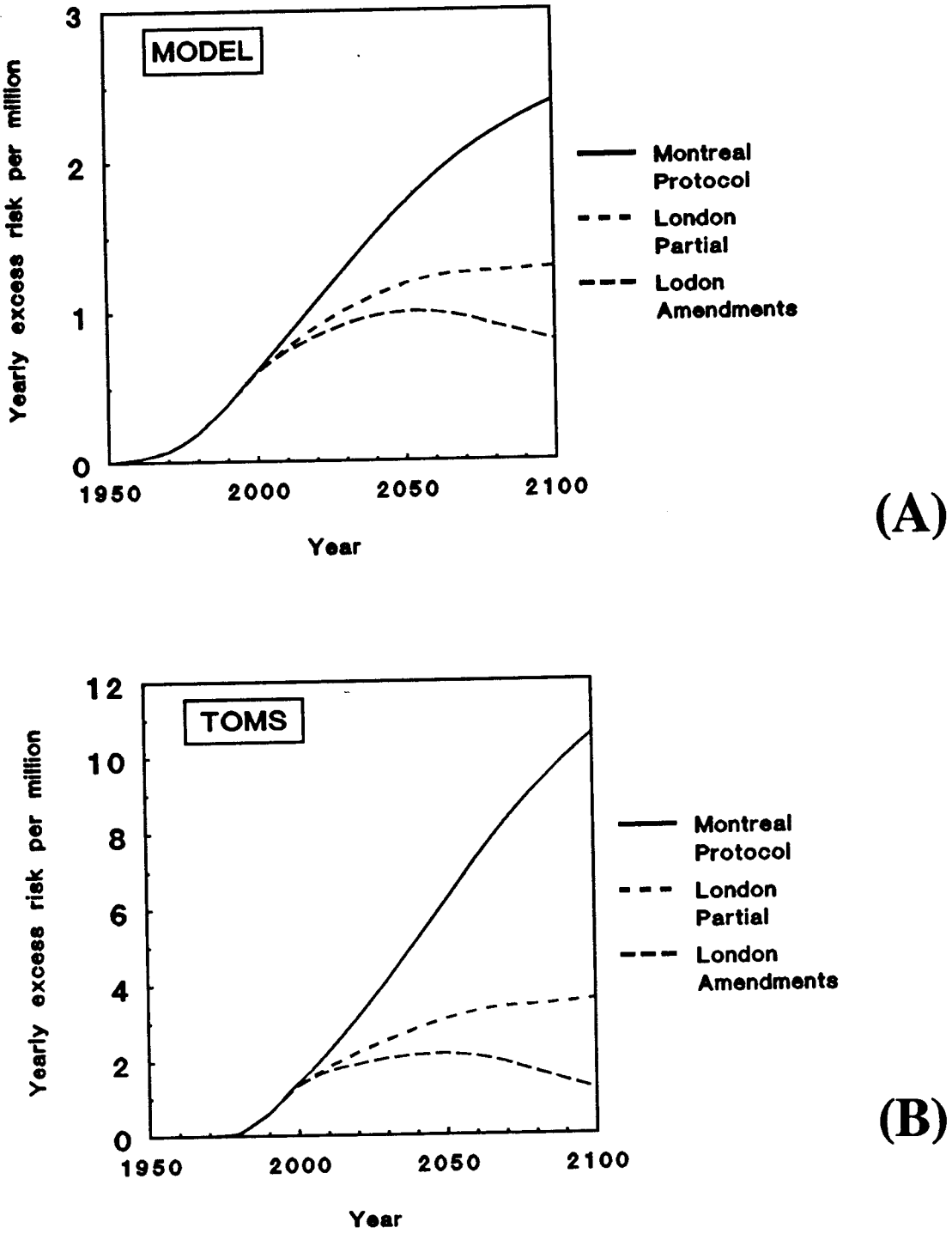

FIG. 3.7 Predicted excess probability of skin cancer deaths in the Netherlands due to ozone depletion, as derived from WMO/UNEP models (A) and TOMS observations (B). Evaluations are based on the 1990 age distribution in the Netherlands.

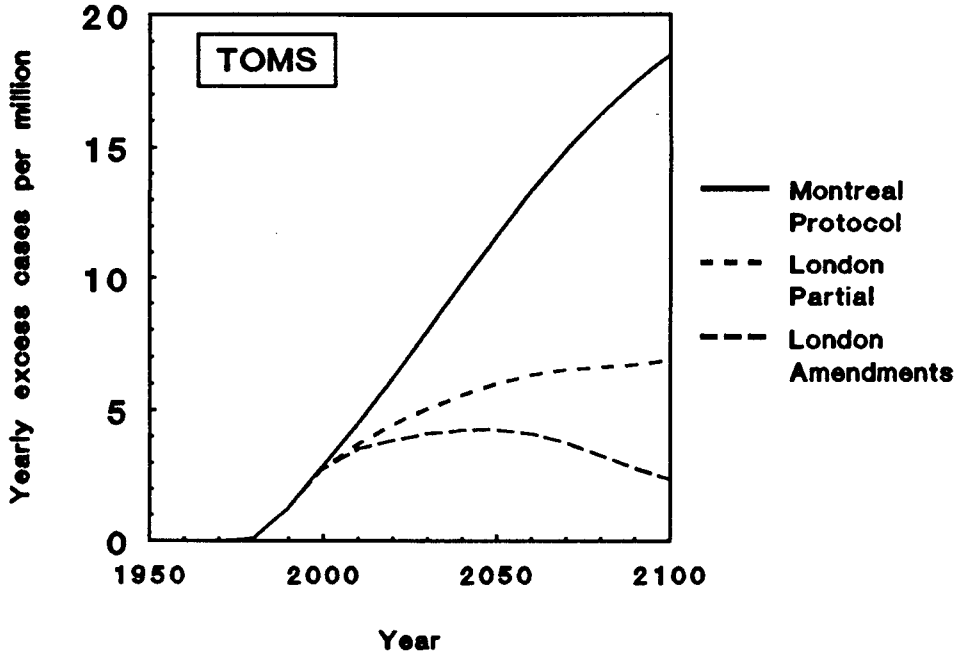

FIG. 3.8 Predicted excess number of melanoma cases, from TOMS measurements. Evaluations are based on the 1990 age distribution in the Netherlands.

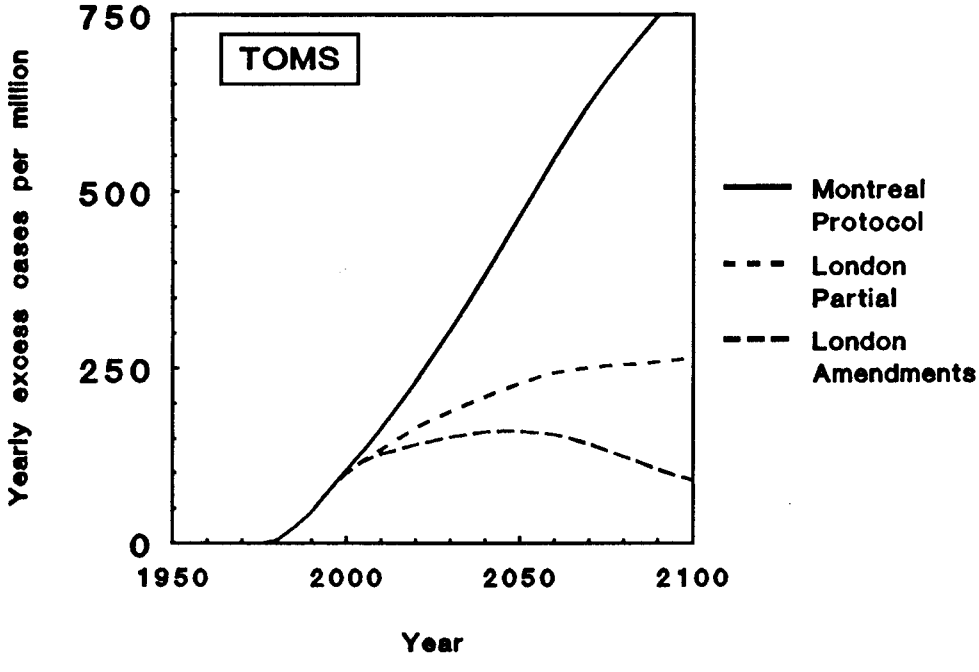

FIG. 3.9 Predicted excess number of non-melanoma skin cancer cases, from TOMS measurements. Evaluations are based on the 1990 age distribution in the Netherlands.

3.4.2 Mortality and incidence of skin cancer in the Netherlands using a population scenario

Skin cancer occurs primarily in older people, and therefore the same UV exposure can lead to higher incidences in an ageing population than in a younger population. Also the expected excess rates due to ozone depletion are dependent on the age distribution in the population. The Dutch population is ageing, therefore even when exposure habits and UV intensities remain unchanged a higher incidence of skin cancer is expected. This is illustrated in Fig. 3.10A, B and C, where the incidence for melanoma, basal cell carcinoma and squamous cell carcinoma respectively are estimated for the period 1950-2050, assuming that no changes in UV exposure occur. We used CBS data on the age distribution of the population for the period 1950-1990, and the mid-scenario for the population over the period 1990-2050 (CBS 1990). As can be seen in the figures a fourfold increase, largely due to ageing is expected over the period covered, since the number of people in the population accounts for maximal a factor of 1.65 (10 million inhabitants in 1950 to 16.5 million in 2025).

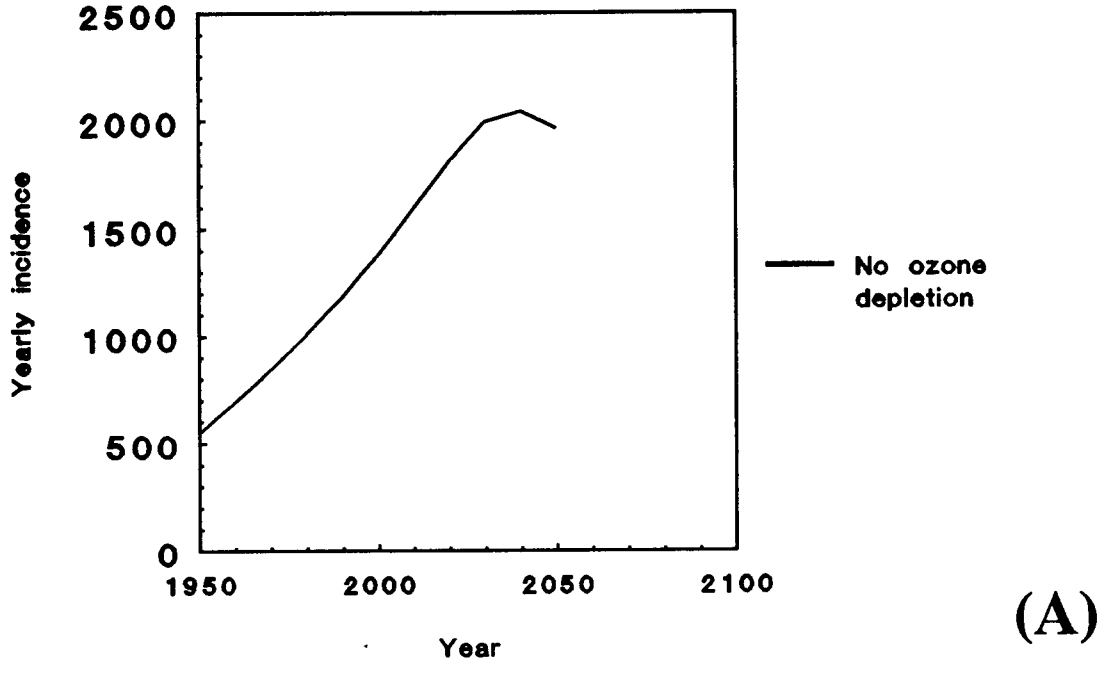

Fig. 3.10 Predicted change in annual number of skin cancer cases due to changes in population size and ageing of the population, assuming that no ozone depletion occurs. Incidences are provided for melanoma (A), basal cell carcinoma (B) and squamous cell carcinoma (C). Evaluations are based on a population scenario for age distribution in the Netherlands.

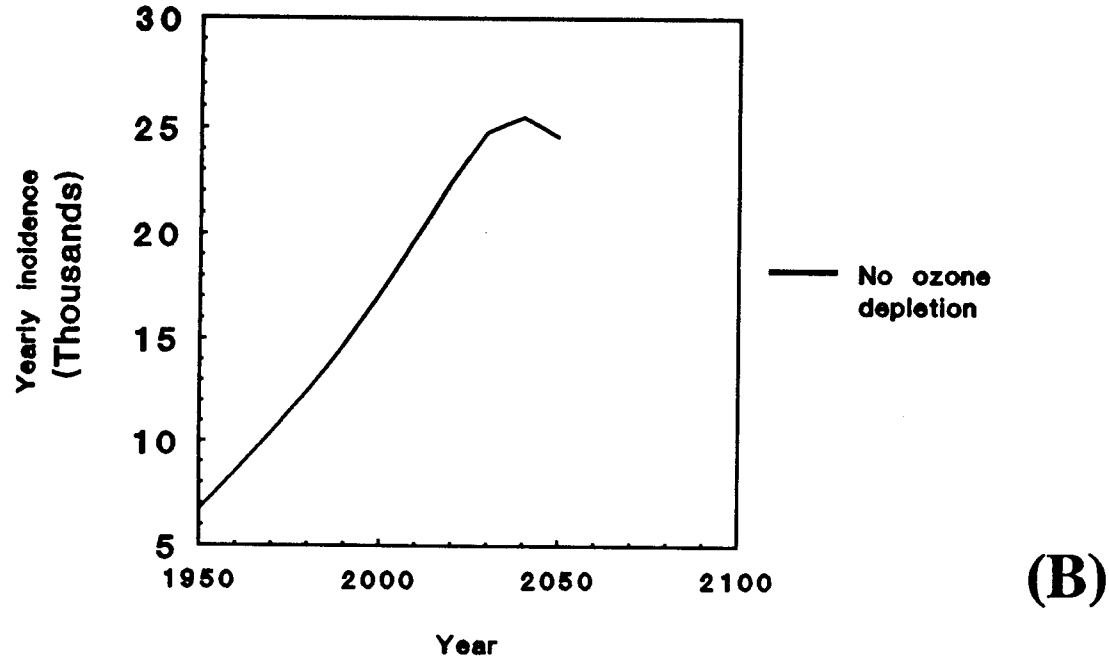

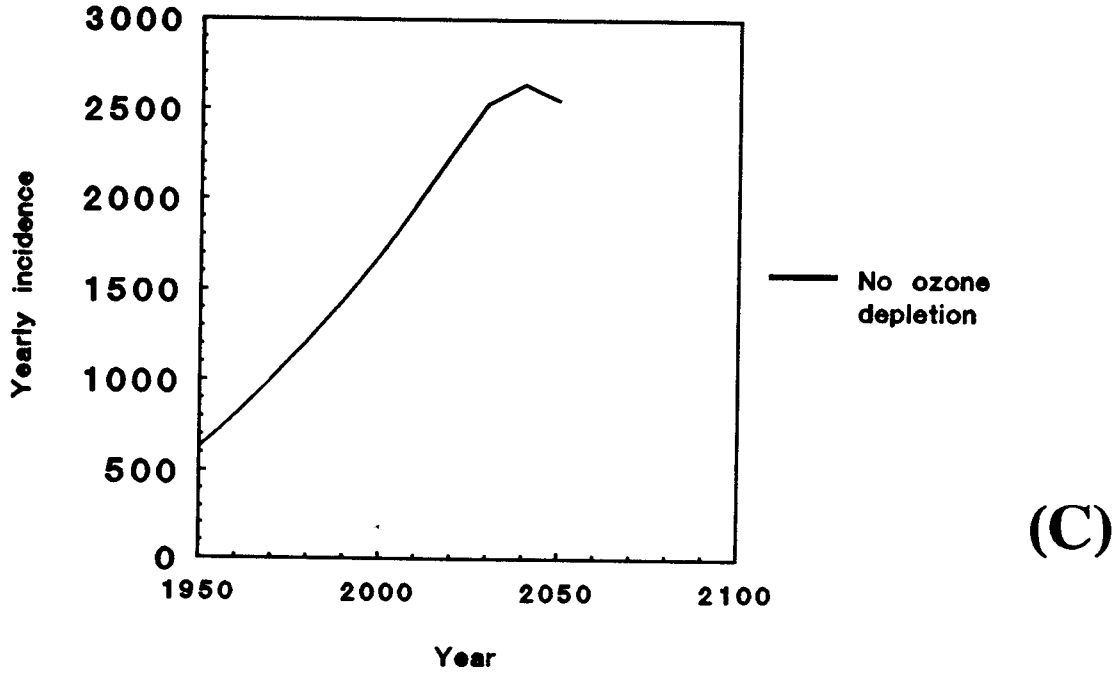

Fig. 3.10 Predicted change in annual number of skin cancer cases due to changes in population size and ageing of the population, assuming that no ozone depletion occurs. Incidences are provided for melanoma (A), basal cell carcinoma (B) and squamous cell carcinoma (C). Evaluations are based on a population scenario for age distribution in the Netherlands.

Excess rates (per million inhabitants), expected due to ozone depletion, are also influenced by the age distribution of the population. The results obtained in Fig. 3.10 are considered as the baseline risks: the incidences occurring when no depletion of ozone occurs. Excess risks, occurring when ozone depletion does occur, are obtained by subtracting the baseline estimates from the total incidences obtained for the various scenarios. Fig. 3.11 provides the TOMS-based calculated excess death rate for the various emission scenarios, taking into account the population scenario. The excess death rates in the year 2050 are approximately 60% higher than the excess death rates calculated for the 1990 population (see previous section): the excess rates in 2050 are estimated at 3.5 per million for the London Protocol and 9.8 per million for the Montreal Protocol. Fig. 3.12 provides the excess number of cases per million for melanoma incidence and Fig. 3.13 gives the results for non-melanoma. Table 3.2 provides the excess incidence and mortality rates for the Netherlands averaged over the period 2000-2050. The full compliance with the London Amendments leads to an approximate twofold reduction in excess rates, as compared to the Montreal Protocol: this is an averaged excess death rate of 2.7 per million per year for the London Amendments, as compared to the 5.3 per million per year for the Montreal Protocol.

TABLE 3.2 Excess skin cancer and mortality rates in the Netherlands averaged over the period 2000-2050

Scenario	Mortality rate (deaths per million per year)	Melanoma incidence (cases per million per year)	Non-melanoma incidence (cases per million per year)
Montreal Protocol	5.3	10.2	395
London Partial	3.4	6.6	247
London Amendments	2.7	5.4	201

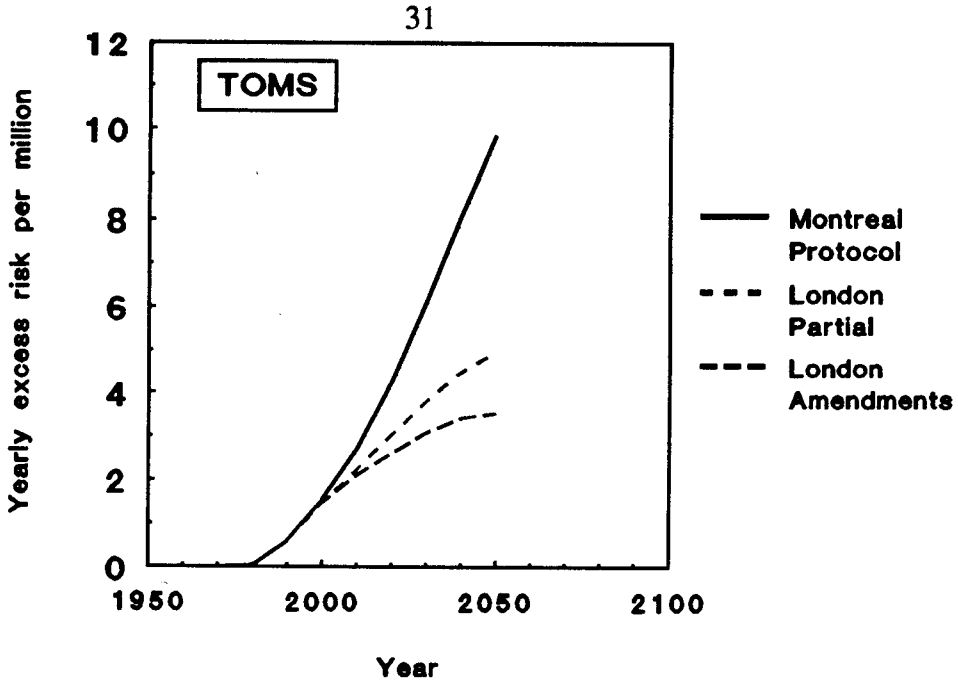

FIG. 3.11 Predicted excess probability of skin cancer deaths in the Netherlands due to ozone depletion, as from TOMS observations. Evaluations are based on a population scenario for the age distribution in the Netherlands.

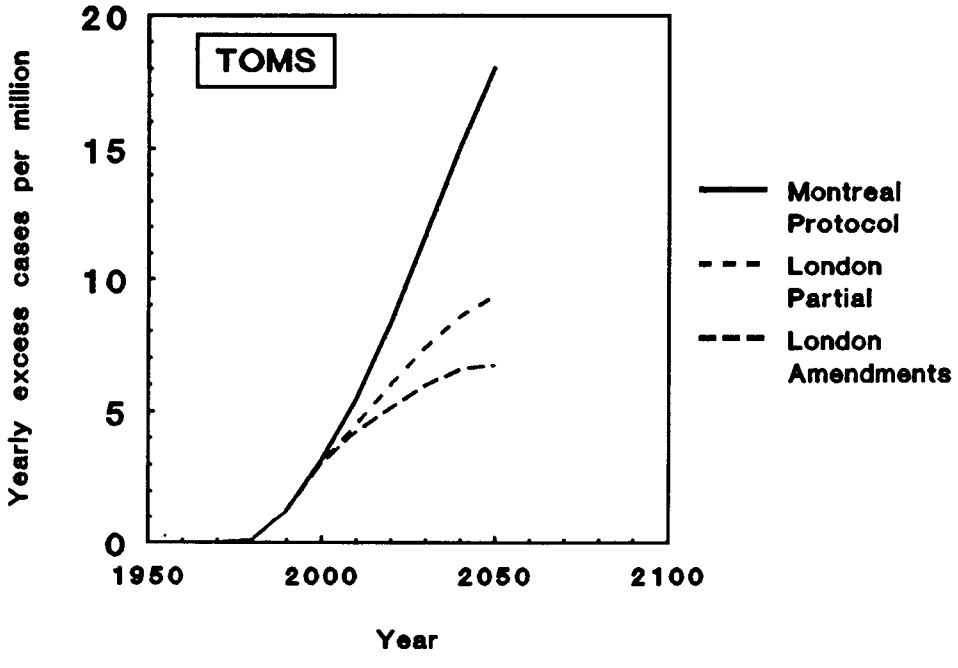

FIG. 3.12 Predicted excess number of melanoma cases from TOMS measurements. Evaluations are based on a population scenario for age distribution in the Netherlands.

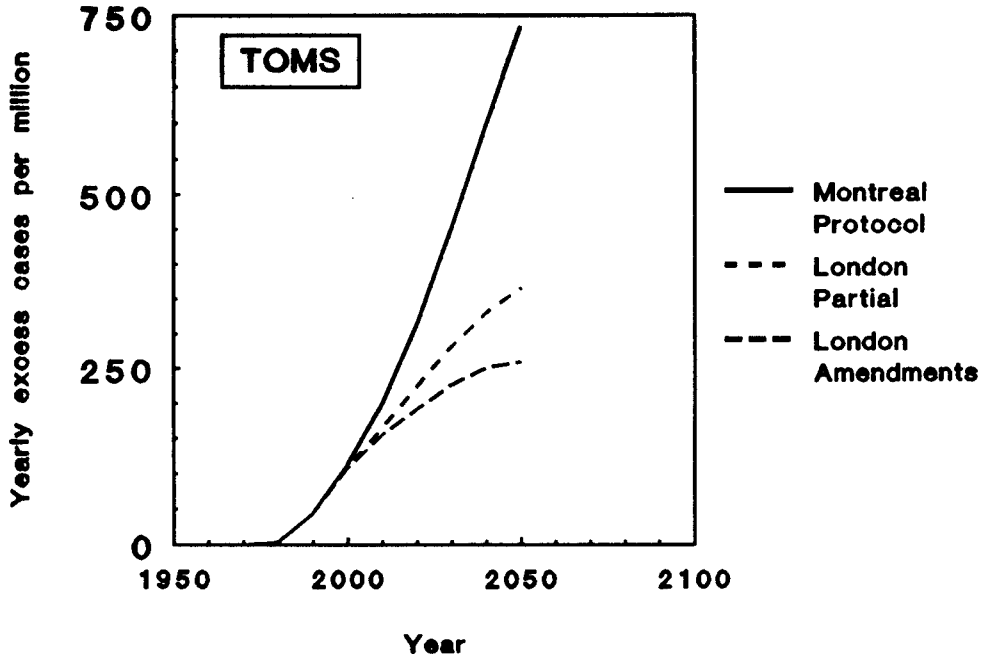

FIG. 3.13 Predicted excess number of non-melanoma skin cancer cases, from TOMS measurements. Evaluations are based on a population scenario for age distribution in the Netherlands.

3.4.3 Global implications for skin cancer incidence and mortality

Ozone depletion has global effects on skin cancer incidence. A full analysis of effects requires detailed information of the global ozone depletion, the geographical and age distributions of the populations at risk, and the present incidences. We are providing preliminary estimates for the effects of ozone depletion on skin cancer incidence and mortality rates in the USA (see Table 3.3), taking into account: the effective UV dose in the USA, the ozone reduction in the USA, and the present skin cancer incidence. In line with assumptions made by UNEP (UNEP, 1991) we can provide some indications of global implications, assuming a worldwide sensitive population of 500 million, with an average UV exposure and skin cancer incidence as observed in the USA (UNEP, 1991). According to these assumptions the excess incidence and mortality rates are equal to the USA estimates in Table 3.3. Multiplying these figures by 500 provides the averaged total number of skin cancer cases and deaths, as provided in Table 3.4.

TABLE 3.3 Excess skin cancer and mortality rates in the USA averaged over the period 2000-2050*

Scenario	Mortality rate (deaths per million per year)	Melanoma incidence (cases per million per year)	Non-melanoma incidence (cases per million per year)
Montreal Protocol	6.6	9.2	616
London Partial Amendments	4.2	5.9	385
London Amendments	3.3	4.9	314

* Preliminary evaluations (see text)

TABLE 3.4 Global yearly excess skin cancer cases and deaths averaged over the period 2000-2050*

Scenario	Skin cancer deaths (yearly)	Melanoma cases (yearly)	Non-melanoma cases (yearly)
Montreal Protocol	3300	4600	310000
London Partial Amendments	2100	3000	190000
London Amendments	1650	2500	160000

* Preliminary evaluations (see text)

4 DISCUSSION

The integrated source-risk model developed in this study is discussed in section 4.1, the results obtained in applying the model are outlined and discussed in section 4.2. In section 4.3 we attempt to provide some perspective in view of the recent (February 1992) commotion on an enhanced depletion.

4.1 Discussion of the model

4.1.1 Integrated modelling approach

Modelling the source-effect chain provides a tool for risk assessment and can thus support risk-oriented policy approaches by comparing effects of various policy options. We have developed a source-effect model for the evaluation of the adverse effects of ozone depletion on skin cancer incidence and mortality. This study is primarily focused on excess risks associated with various emission scenarios for ozone-depleting substances (section 3.4). The model can also be applied to estimate effects of an ageing population (section 3.4.2) or changing exposure habits.

The estimation of risks associated with the emission of halocarbons has been addressed by various other studies, however, an integrated approach as presented in this report is lacking. Previous studies have primarily focused on aspects of the source-risk chain: either the dispersion and atmospheric chemistry (WHO/UNEP, 1989; Stolarski et al., 1991), the increases in effective irradiance in relation to ozone depletion (Kelfkens et al., 1991; UNEP, 1991), or the dose-response relationship of skin cancer incidence (Scotto et al., 1982; De Gruijl et al., 1982; Rundel, 1983; Slaper et al., 1986; Moan, 1991). Attempts to integrate (UNEP, 1989; UNEP, 1991; Rundel, 1983B; Moan, 1991) do not fully account for the delay mechanisms involved in the source-risk chain:

- delay between production and emission,
- delay due to long atmospheric lifetimes of halocarbons, the slow dispersion to the stratosphere and chemical balances,
- delay due to the fact that effects are related to long term exposure.

We have used the results previously obtained in various detailed studies and incorporated the delay times for the various processes.

Although our aim was to obtain reliable 'state-of-the-art' evaluations of the future effects of ozone depletion, it is realised that model evaluations provide estimates and therefore uncertainties. The history on the evaluation of ozone depletion has shown several major occurrences of unexpected phenomena:

- the discovery of the Antarctic ozone hole in 1985 was according to models, unexpected;
- measurements of ozone depletion have shown a much larger depletion than expected, as based on model evaluations of atmospheric chemistry
- the surprisingly high concentrations of chlorine in the stratosphere above Europe and the USA, as discovered in the winter of 1992, were not predicted by models.

It is therefore important that in combination with modelling efforts, which aim at prognosis of environmental quality, monitoring efforts are continued and strengthened.

4.1.2 Production and emission

Two of the three production scenarios used in this study were adopted at international conferences (Montreal Protocol, adopted in 1987 and further strengthened in the London Amendments in 1990). It is not clear to what extent non-subscribing countries will limit or reduce their emissions. We therefore included a third scenario, in which the London Amendments are not fully implemented. All scenarios assume at least 50% reduction in production of the primary CFC's, as compared to the 1986 production level. The recent alarming publicity on unexpected high levels of active chlorine above large parts of the Northern Hemisphere, has led to policy discussions on faster implementation of reduction scenarios. Possible implications are discussed in section 4.3.

4.1.3 Atmospheric dispersion and chemistry

Using currently available model evaluations, based on atmospheric chemistry, we expect an approximate 1% decrease in ozone for each 1 ppbv increase in stratospheric chlorine. Satellite-based measurements (TOMS) have shown a decrease of 4-5% per ppbv (see Table 2.2). We have therefore provided estimates based on the results of complicated atmospheric models, as well as estimates based upon the extrapolation of satellite measurements of ozone depletion. In view of the fact that atmospheric chemistry is very complicated, and not completely understood, we have used primarily the TOMS measurements for the estimation of effects. The model-based estimates provide 2-4 times lower risks than the TOMS-based estimates (compare Fig. 3.7A and 3.7B).

4.1.4 Atmospheric UV transfer

Systematic UV measurements are largely lacking (UNEP, 1991). We have used results obtained with a previously developed model for atmospheric UV transfer (De Leeuw, 1988), which was found to be in line with the limited measurement data available at present (De Leeuw and Slaper, 1990). The calculations were made for the situation that other atmospheric parameters influencing UV irradiance, like cloudcover, aerosol content, albedo and tropospheric ozone remain constant over the calculation period. In contrast with many other studies (UNEP, 1991), we incorporated the seasonal variations of total column ozone and ozone depletion in our calculations of the biologically effective UV dose.

In order to estimate the risks of increases in UV exposure, one has to use proper weighting functions and dose-effect relationships. We have used an action spectrum previously determined for induction of skin tumors in the hairless mouse (Slaper, 1987). The action spectrum is roughly similar to the erythema action spectrum in humans, and has previously been adopted by UNEP (UNEP, 1989). An improved action spectrum is now developed, but deviations regarding the effects of ozone depletion are probably less than 10% (UNEP, 1991).

4.1.5 Dose-effect relationship

Regarding the dose-effect relationship for non-melanoma, each per cent increase in long term UV exposure is expected to lead to 1.5% additional basal cell carcinomas, and 2.5% additional squamous cell carcinoma. These estimates are in line with those provided in UNEP, 1991: 1.4% for basal cell carcinoma and 2.5% for squamous cell carcinoma. The present incidence of non-melanoma skin cancer in the Netherlands is not very well-known. We estimated a total of 16,500 cases per year. The incidence figures could be off by 10-30%, however, the present death-rate is better known (80-90 deaths per year).

With respect to melanoma skin cancers the relationship between UV exposure and incidence is somewhat ambigious. No action spectrum has been determined and the fraction of UV-induced melanoma is not clear. We assumed that the action spectrum for melanoma induction is similar to the action spectrum for the induction of non-melanoma skin cancers. Dose-response parameters have been estimated on the basis of epidemiological data obtained at various latitudes in the USA (EPA 1987). A 1% increase in UV is assumed to lead to 0.6% increase in melanoma incidence. The age dependency was estimated on the basis of age-specific incidence figures, taking into account the differences found between various birth cohorts.

Melanoma incidence has risen globally over the past decades. The increase is much larger than expected on the basis of the changes in size and age distribution of the population. Observed mortality rates for melanoma in the Netherlands increased at least sevenfold, from 3 per million per year in 1950 to 20 per million per year in 1990. An increase by a factor of 1.5-2 can be explained due to ageing of the population. Ozone depletion over the past decades also provides an insufficient explanation, since an increased mortality rate of maximally 0.3 per million per year was expected. It has been assumed that sunshine holidays are a major factor in the rising melanoma incidence, however, the evidence on this hypothesis is conflicting (UNEP, 1991; UNEP, 1989). Recent trend analysis of melanoma death rates by cohorts in the USA provided evidence that the rise in melanoma death rates will discontinue (Scotto et al., 1991). If no further change in lifestyle, or ultraviolet exposure, occurs a downward trend is expected after the second decade of the 21st century (Scotto et al., 1991). In view of the uncertainties we have not included cohort effects in our estimates. We have chosen to take the present exposure habits and lifestyle as a baseline for our risk estimates: changes in behaviour can of course seriously influence the future incidences and death rates.

4.2 Summary of results

The results obtained applying the chain model show that further ozone depletion will occur over the next decade and full recovery of the ozone layer is not expected in the next century, even if the London Amendments are fully implemented on a global schale (Fig. 3.5). The three scenarios considered indicate similar depletions for the next decade, however, large differences will occur in the next century. The Montreal Protocol indicates a continuing decrease of ozone throughout the next century: 24% depletion in 2100 (according to TOMS-based estimates), whereas a depletion of 2% in 2100 is expected if the London Amendments are fully implemented.

The estimated effects of ozone depletion on skin cancer mortality and incidence are summarised in tables 4.1, 4.2 and 4.3 for the Montreal Protocol and for the London Amendements. Excess rates only include additional cases, due to ozone depletion. If the London Amendments are fully implemented an increase in excess death rate from 1.5 per million per year around the year 2000 to 2-4 per million per year around 2050 is expected, followed by a slight decrease remaining just above 1 per million per year in 2100. The Montreal Protocol leads to increasing death rates throughout the entire century: 6-10 per million in 2050 and more than 11 per million in 2100. The excess death and incidence rates found for the London Amendments are substantially lower than those for the Montreal Protocol: three times lower in 2050 and nearly 10 times lower in 2100.

TABLE 4.1 Excess[#] skin cancer death rates in the Netherlands due to ozone depletion

Protocol	Population	Deaths per million per year (n) in 2000	Deaths per million per year (n) in 2050	Deaths per million per year (n) in 2100
LONDON AMEND-MENTS	1990	1.4	2.2	1.2
	scenario	1.5	3.5	ND *
MONTREAL PROTOCOL	1990	1.4	6.2	10.6
	scenario	1.5	9.8	ND *

[#] Excess rates refer to additional cases of skin cancer, which are due to ozone depletion
* Not determined

TABLE 4.2 Excess[#] melanoma skin cancer cases in the Netherlands due to ozone depletion

Protocol	Population	Cases per million per year (n) in 2000	Cases per million per year (n) in 2050	Cases per million per year (n) in 2100
LONDON AMEND-MENTS	1990	2.8	4.3	2.4
	scenario	3.1	6.7	ND *
MONTREAL PROTOCOL	1990	2.9	11.6	18.5
	scenario	3.2	18.1	ND *

[#] Excess rates refer to additional cases of skin cancer, which are due to ozone depletion
* Not determined

TABLE 4.3 Excess[#] non-melanoma skin cancer cases in the Netherlands due to to ozone depletion

Protocol	Population	Cases per million per year (n) in 2000	Cases per million per year (n) in 2050	Cases per million per year (n) in 2100
LONDON AMEND-MENTS	1990	99	161	89
	scenario	108	258	ND *
MONTREAL PROTOCOL	1990	103	464	801
	scenario	112	734	ND *

[#] Excess rates refer to additional cases of skin cancer, which are due to ozone depletion
* Not determined

The estimated rates provided in this study are population based averages. Within the population specific risk groups, like for example people with a UV sensitive skin and/or high UV exposure (workers in outdoor occupation) are expected to have considerably higher excess rates.

Averaged over the period 2000-2050 the yearly excess mortality and incidence rates are nearly twofold lower for the London Amendments, as compared to the Montreal Protocol. For the Dutch population we find 2.7 versus 5.3 deaths per million per year, 5.4 versus 10.2 melanoma cases per million per year and 200 versus 395 non-melanoma skin cancer cases per million per year (Table 3.2).

Comparing the estimates for the Netherlands with preliminary estimates for the USA shows that averaged over the period 2000-2050: excess mortality rates are 20-25% higher in the USA, excess incidence rates for melanoma 10% less and excess incidence rates for non-melanoma 55% higher (Table 3.3). Rough estimates for the global implications in the period 2000-2050 show that for the Montreal Protocol 3300 additional deaths per year are expected, 4600 excess cases of melanoma and over 300,000 cases of nonmelanoma. Full implementation of the London Amendments reduces these estimates approximately twofold. It should be noted that these global estimates are problably conservative (UNEP, 1991).

4.3 Recent developments on ozone depletion and policies

4.3.1 An enhanced depletion of the ozone layer?

The recent findings of surprisingly high concentrations of active chlorine in the stratosphere in large parts of the Northern Hemisphere has led to expectations that under unfavourable weather conditions ozone depletion in 1992 might be 30-40% during the early spring months at high and mid-latitudes. This is a reduction which is at least four times worse than the previously observed trends in ozone depletion in early spring (typically around 8% as in Fig. 2.3). It is at present not clear whether such large depletions will actually occur. Observations of ozone in the spring of 1992 have not revealed the enhanced depletion. Nevertheless, the possibility of an 'enhanced' depletion poses questions regarding the possible consequences and effects of the alarming findings.

It has been indicated that the surprisingly high concentrations of active chlorine were caused by CFC emissions over the past decades, in combination with the sudden increase of stratospheric dust due to the volcanic eruption of the Pinatubo in the summer of 1991 (NASA, 1992). If so, it is expected that an 'enhanced' depletion will not last more than a decade at the most.

Although somewhat speculative, we have tried to estimate the consequences of a sudden strong depletion over a period of 3-10 years. If ozone is reduced by 30-40%, the effective UV irradiance is expected to increase by 60-70%, assuming that stratospheric dust has little effect on UV transfer in the atmosphere. For risk assessments it is most important to assess the increases in UV exposure during the summermonths, since 75% of the yearly effective UV-burden is received in the period May-August, as compared to only 10% in the period Februari-April. Analogous with the observed trends in ozone depletion in the Northern Hemisphere over the past decade (at present 8% in the early spring and 2% in the summer period) and the observations regarding the Antarctic ozone hole, it seems plausible that the

depletion will be less during the summer. An average extra depletion of 20% throughout the year is probably an upper estimate. According to our model evaluations the associated upper estimate for the increase in year-round UV exposure is 30%. If the 'enhanced' depletion is restricted to the winter and early spring months, the estimated additional year round UV burden is 5-10%.

We investigated the possible effects of an additional UV burden, assuming a linear decline to zero over a period of 10 years and 3 years. In case of a decline over a period of 10 years, the additional UV dose received amounts to an upper estimate of 1.5 times the 'normal' UV-burden for a year (annual dosis) for a year-round depletion, and 0.25-0.5 times the annual doses for an early spring depletion.

The additional death rates in the Netherlands associated with the above-mentioned 'enhanced' exposures amount to 0.4-0.5 per million per year around the year 2000 for the highest additional UV dose (1.5 annual dosis). This estimated risk will slowly decrease to 0.3 per million per year in 2050, 0.13 in 2070 and 0 in 2100. If the recovery from the 'Pinatubo enhancement' occurs within three years, the estimated excess risk is 0.14 deaths per million per year around 2000. If the enhanced depletion is restricted to early spring the additional death rates will amount to 0.11 around 2000, and 0.04 per million per year for 10 and 3-year recovery periods respectively.

If the enhancement occurs, these death-rates will add to the risk estimated in our previous analysis. Comparing the upper estimates given above to the excess risks estimated in our previous analysis in Table 4.1, we can see that around 2000 the Pinatubo enhancement amounts to maximally approximately 30% of the expected excess risk in our previous calculations, decreasing to 10-15% around the year 2050, and to less than 10% after 2070. The results of this analysis must be regarded with caution, since it is not certain that the expected depletion will occur, and furthermore, the recovery of this effect is uncertain. We can conclude, however, that at present the risks of the continuing ozone depletion will most probably be larger than the effects of the enhanced depletion over a short time period. However, monitoring chlorine, ozone and UV irradiance at ground level has in view of the uncertainties considerable importance.

4.3.2 Effects of new policies

The USA and EC have recently decided to aim at a full production stop of the principal ozone-depleting substances in 1995. These countries cover roughly two-thirds of the world-use CFC's (Den Elzen et al., 1990; UNEP, 1989B). If global implementation of these countermeasures is achieved, a preliminary evaluation shows an additional 20-30% reduction in excess skin cancer cases in the period 2000-2050, when compared with the London Amendments. However, such a reduction is only achieved if all countries in the world comply and an enhanced depletion (as indicated in section 4.3.1) can limit the decreasing effects.

5 CONCLUSIONS

A source-effect model has been developed for the prognosis of the incidence of skin cancer in relation to emission scenarios for ozone-depleting substances. The model is used to estimate tropospheric concentrations of CFC's, chlorine levels in the stratosphere, ozone depletion, UV irradiance and effects on skin cancer incidence and death rates. The model provides a tool to support risk-oriented policy approaches regarding the depletion of the ozone layer. The results obtained using the model show that depletion of the ozone layer is expected to continue far into the next century, despite the fact that a considerable reduction of emissions of ozone-depleting substances is assumed in all three scenarios considered. In fact no full recovery of the stratospheric chemical balance is expected in the next century, even if all the countries in the world comply with the London Amendments of the Montreal Protocol.

We calculated the excess incidence and mortality rates for skin cancer for three CFC-emission scenarios: the fully implemented Montreal Protocol (MP), the fully implemented London Amendments (LA), and the partially implemented London Amendments (LP). The excess rates refer to the extra cases (and deaths) which can be attributed to ozone depletion. The excess rates do not include the cases expected in the absence of ozone depletion. Regarding the effects on skin cancer death rates in the Netherlands an excess death rate of at least 1 per million per year is expected throughout the next century for the three scenarios. The excess rates depend on the age distribution of the population. Therefore two sets of calculations were performed for the three scenarios: one set using a constant age distribution of the population (1990 age distribution for the Netherlands), and one using a population scenario for the Netherlands (upto 2050). Results obtained applying the population scenario (upto 2050) are indicated below in brackets . The full compliance with the Montreal Protocol is expected to lead to an increasing excess death rate of 1.4 (1.5) per million per year in 2000, 6.2 (9.8) per million per year in 2050 and 10.6 per million in the year 2100. Full compliance with the London Amendments shows a maximum excess death rate of 2.2 (3.5) per million per year in the year 2050, slightly decreasing to 1.2 per million in 2100. The total excess skin cancer incidence rates show the same pattern, but are considerably higher than the death rates. For the MP we find excess rates increasing throughout the next century: 110 (115) per million per year around 2000, 475 (750) per million per year in 2050 and 820 per million per year in 2100. For the LA scenario we find: 100 (110) per million per year in 2000, 165 (265) per million per year in 2050 and 90 per million per year in 2100.

We conclude that the excess death and incidence rates predicted for the London Amendments are substantially lower than those for the Montreal Protocol: three times lower in 2050, and nearly 10 times lower in 2100. For all scenarios the excess rates are higher when using the population scenario, compared to the calculations using the constant 1990-population; the difference is nearly 10% in 2000 and increases to nearly 60% in 2050. Ageing of the Dutch population causes these differences, and is also expected to lead to an increase in the overall incidence if no depletion of the ozone layer would occur. The estimates show that due to ageing of the population the total number of skin cancer cases is expected to increase 60-70%: from 18000 (1200 per million) per year at present to 30000 (nearly 2000 per million) around 2040. The effects of ozone depletion as indicated by the presented excess rates adds to this increase.

Averaged over the period 2000-2050 the yearly excess mortality and skin cancer incidence rates are nearly two times lower for the London Amendments (LA), as compared to the Montreal Protocol (MP). For the Dutch population scenario, we find 50-year averages of 2.7 (LA) versus 5.3 (MP) deaths per million per year, 5.4 (LA) versus 10.2 (MP) melanoma cases per million per year and 200 (LA) versus 395 (MP) non-melanoma skin cancer cases per million per year.

Comparing the estimates for the Netherlands with preliminary estimates for the USA shows that averaged over the period 2000-2050 excess mortality rates are 20-25% higher in the USA; excess incidence rates for melanoma are 10% lower and for non-melanoma are 55% higher. Crude estimates for the global implications in the period 2000-2050 show that for the Montreal Protocol: 3300 additional deaths, 4600 excess cases of melanoma, and over 300,000 cases of non-melanoma are expected per year. Full implementation of the London Amendments reduces these estimates approximately twofold. It should be noted that these worldwide estimates are problably conservative.

In view of the alarming figures on chlorine levels in Europe and the USA, as observed this winter (1992), further enhancement of ozone depletion is expected in the spring. Although a detailed explanation of the observations is lacking, it has been speculated that stratospheric dust from the volcanic eruption of the Pinatubo is enhancing the effects of CFC emissions over the last decades. If this enhancement occurs, it will probably be an effect for the next few years to a decade. An upper estimate for the possible effects on skin cancer death rate indicates 0.4-0.5 deaths per million per year at the beginning of the next century (slowly decreasing afterwards). Although these results must be considered with caution due to the large uncertainties in the present developments, it seems likely that the continuing ozone depletion has larger adverse effects than the sudden enhancement that might occur due to Pinatubo. Careful monitoring of ozone and UV irradiance should further substantiate these findings.

The model provided in this study can be used to support evaluations of further policy options, including the role of CFC alternatives. Furthermore, the model could provide a supportive tool in the determination of scenarios leading to sustainable development with regard to the ozone layer. Other effects of ozone depletion on human health or aquatic and terrestric ecosystems could also be included in the model, provided that sufficient information on exposure-effect relationships becomes available.

6 REFERENCES

Bowman K.P. (1985) A global climatology of total ozone from the Nimbus-7 total ozone mapping spectrometer. In: Atmospheric Ozone, (edited by C.S. Zerefos and A. Ghazi), Reidel, Dordrecht, pp. 363-367.

CBS (1990) Central Bureau of Statistics.

CMA (1987) (Chemical Manufacturers Association), (1987) Production, sales and calculated release of CFC-11 and CFC-12 through 1986, News release of the CMA, Washington DC, 18 November 1987.

CMA (1988) Production, sales and calculated release of CFC-11 and CFC-12 through 1987, News release of the CMA, Washington DC.

De Gruijl F.R. and van der Leun J.C. (1980) A dose response model for skin cancer induction by chronic UV exposure of a human population: J.Theor. Biol., 83 487-504:

De Gruijl F.R. (1987) The dose response relationship for UV-tumorigenensis: PhD thesis, State University of Utrecht.

De Leeuw F.A.A.M. (1988) Modelmatige berekening van fotolyse snelheden relevant voor troposferische chemie, RIVM rapport nr. 228603003, Bilthoven The Netherlands.

De Leeuw F.A.A.M. de, and Slaper H. (1989) UV Straling in Nederland: indicatie van de invloed van een verandering in de ozonkolom, RIVM rapport nr. 228903001 Bilthoven The Netherlands.

Den Elzen M.G.J., Rotmans J. and Swart R.J. (1990) The role of CFC's, substitutes and other halogenated chemicals in climate change. RIVM Report no. 222901002 Bilthoven, The Netherlands July 1990.

Den Elzen M.G.J. Swart R.J. and Rotmans J. (1992) Strengthening the Montreal Protocol: does it cool down the greenhouse; The Science of the Total Environment. In press.

EPA (1987) Ultraviolet radiation and melanoma; with a special focus on Assessment of the risks of stratospheric ozone depletion, EPA 400/1-87/001D, December 1987.

EPA (1988) Future concentrations of stratospheric chlorine and bromine, Washington DC, EPA 400/1-88-005, 1988.

EPA (1990) Reducing risk: setting priorities for environmental protection, Science Advisory Board of EPA, September 1990.

Gamlen P.H. Lane B.C. Migley P.M. and Steed J.M. (1986) The production and release to the atmosphere of CCl_3F and CCl_2F (CFC-11 and CFC-12), Atmospheric Environment, 20, 1077-1085.

GEMS (1989) GEMS Monitoring and Assessment Research Centre, Environmental data report, UNEP London (UK) in cooperation with the World Resources Institute, Washington DC and UK Department of the Environment, 1989.

Gezondheidsraad (1986) Human exposure to ultraviolet radiation, Report 1986/9E, 's Gravenhage.

IPCC (1990) Emission scenarios for the response strategies working group of the Intergovernmental Panel on Climate Change; Report of the expert Group on emission scenarios, Washington DC.

Kelfkens G., de Gruijl F.R. and van der Leun J.C. (1990) Ozone depletion and increase in annual carcinogenic ultraviolet dose. Photochem. Photobiol, 52, 819-23.

Lovelock J.E. (1973) Halogenated hydrocarbons in and over the Atlantic, Nature, 241, 194-196.

Moan J. (1991) Ozone hole and biological consequences. J. Photochem. Photobiol., 9, 244-247.

Molina J.M. and Rowland, F.S. (1974) Stratospheric sink for chlorofluoromethanes: chlorine atom-catalysed destruction of ozone, Nature, **249**, 810-812.

NASA (1992) Ozone depletion a possibility over northern populated areas; releases 92-18 and 92-19, NASA News February 1992.

Neering H. and Cramer M.J. (1988) Nederlands Tijdschrift Geneeskunde 132, 1330-1333.

Parrish J.A., Jaenicke K.T. and Anderson RR (1982) Photochem. Photobiol, 36, 187-191.

Prather M.J. and Watson RT (1989) Transient scenarios for atmospheric chlorine and bromine, NASA Headquarters, Washington DC.

Rotmans J. (1990) IMAGE, An Integrated Model to Assess the Greenhouse Effect, Kluwer Academic, Dordrecht, The Netherlands, ISBN 0-7923-0957-X.

Rundel R.D. and Nachtwey D.S. (1983) Promotional effects of ultraviolet radiation on human basal and squamous cell carcinoma. Photochem. Photobiol., 38, 569-575.

Rundel R.D. (1983) Photochem. Photobiol, 38, 577-591.

Scotto J., Fears T.R. and Fraumeni J.F. (1981) Incidence of non-melanoma skin cancer in the United States, US Department of Health and Human Services, NIH 82-2433.

Scotto J., Pitcher H. and Lee J.A.H. (1991) Indications of future decreasing trends in skin-melanoma mortality among whites in the United States, Int. J. Cancer, 49, 1-8.

Slaper H., Schothorst A.A. and van der Leun J.C. (1986) Risk evaluation of UVBN therapy for psoriasis: comparison of calculated risk for UVB therapy and observed risk in PUVA-treated patients, Photodermatology, 3, 271-283.

Slaper H. (1987) Skin cancer and UV exposure: investigations on the estimation of risks, PhD thesis, State University of Utrecht

Slaper H. and Eggink G.J. (1991) Blootstelling aan ultraviolette straling; een analyse van het probleemveld, RIVM rapport nr. 249104002 Bilthoven The Netherlands (summary in English).

Sterenborg H.J.C.M. (1987) Investigations on the action spectrum of tumorigenesis by ultraviolet radiation, PhD-thesis, State University of Utrecht.

Stolarski R.S., Bloomfield P., McPeters R.D. and Herman J.R. (1991) Total ozone trends from NIMBUS-7 TOMS data, J. Geophys. Res. Lett., **18**, 1015-1018.

UNEP (1989) Environmental Effects Panel Report, Pursuant to Article 6 of the Montreal Protocol on Substances that deplete the ozone layer under Auspices of the UNEP, November 1989.

UNEP (1991) Environmental Effects of ozone depletion. Panel Report Pursuant to Article 6 of the Montreal Protocol on Substances that deplete the ozone layer under Auspices of the UNEP, November 1991.

VROM (1989) Omgaan met risico's, de risicobenadering in het milieubeleid. Ministerie van Volkshuisvesting Ruimtelijke Ordening en Milieubeheer, 's Gravenhage.

Wigley T.M.L. (1988) Future CFC concentrations under the Montreal Protocol and their greenhouse-effect implications, Nature 335, 333-335.

WMO/UNEP (1989) Scientific Assessment of Stratospheric Ozone 1989, Report No. 20, Volume I.